HHS Public Access

Author manuscript

J Med Chem. Author manuscript; available in PMC 2024 February 23.

Published in final edited form as:

J Med Chem. 2023 February 23; 66(4): 2904–2917. doi:10.1021/acs.jmedchem.2c01941.

Development of Substituted Phenyl Dihydrouracil as the Novel Achiral Cereblon Ligands for Targeted Protein Degradation

Haibo Xie[1,‡], **Chunrong Li**[1,‡], **Hua Tang**[1], **Ira Tandon**[1], **Junzhuo Liao**[1], **Brett L. Roberts**[1], **Yu Zhao**[1], **Weiping Tang**[1,2]

[1]Lachman Institute for Pharmaceutical Development, School of Pharmacy, University of Wisconsin-Madison, 777 Highland Avenue, Madison, WI 53705 (USA)

[2]Department of Chemistry, University of Wisconsin-Madison, 1101 University Avenue, Madison, WI 53706 (USA)

Abstract

Glutarimides such as thalidomide, pomalidomide, and lenalidomide are the most frequently used ligands to recruit E3 ubiquitin ligase cereblon (CRBN) for the development of proteolysis targeting chimeras (PROTACs). Due to the rapid and spontaneous racemization of glutarimides, most CRBN-recruiting PROTACs are synthesized as a mixture of racemates or diastereomers. Since the (*S*)-enantiomer is primarily responsible for binding to CRBN, the existence of the largely inactive (*R*)-enantiomer complicates the drug development process. Herein, we report that substituted achiral phenyl dihydrouracil (PDHU) can be used as a novel class of CRBN ligands for the development of PROTACs. Although the parent PDHU has minimal binding affinity to CRBN, we found that some substituted PDHUs had comparable binding affinity to lenalidomide. Structural modeling provided further understanding of the molecular interactions between PDHU ligands and CRBN. PDHUs also have greater stability than lenalidomide. Finally, potent BRD4 degraders were developed by employing trisubstituted PDHUs.

Graphical Abstract

Corresponding Author: Weiping Tang, weiping.tang@wisc.edu.

Author Contributions

W.T. conceptualized and directed the project. W.T. and H.X. drafted the manuscript with the assistance from other co-authors. H.X. designed and conducted most chemistry experiments and binding assay. C.L. designed and conducted most biology experiments. H.T. prepared compounds 12B and 12C. I.T. tested compound 13 in Flp-In™-293 cells. J. L. performed the computational modeling and provided the rationalization for the SAR. B.R. and I.T. developed the Flp-In™-293 cell line. Y.Z. prepared the unsubstituted PDHU 2.

‡These authors contributed equally.

Supporting Information. This material is available free of charge via the Internet.

Compound **6F** binding poses modeling, human plasma, human liver microsome and hydrolysis stability, fluorescence polarization binding assays, HPLC traces, NMR spectra (PDF).

Molecular formula strings (CSV).

A patent application for some compounds in this manuscript was filed.

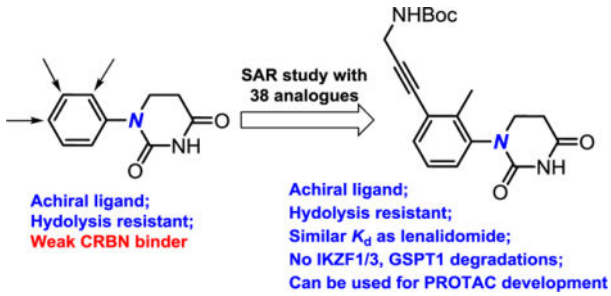

Keywords

PROTAC; cereblon; dihydrouracil; thalidomide; lenalidomide

Introduction

Targeted protein degradation has recently emerged as a promising modality for the development of therapeutics to address numerous unmet medical needs.[1–5] Proteolysis targeting chimera (PROTAC) is the most well-known strategy for the degradation of intracellular protein targets.[6] PROTACs are bifunctional molecules that are composed of a E3 ubiquitin ligase binding motif, a linker, and a protein of interest (POI) binding motif. PROTACs can serve as a molecular adapter to induce the interactions between the POI and the E3 ligase, which in turn promotes polyubiquitination and subsequent proteasomal degradation of the POI.[7] Although there are over 600 E3 ubiquitin ligase complexes in human proteome, few of them have been employed for the development of PROTACs.[1] Among them, CRBN is the most frequently utilized E3 ligase due to the low molecular weight and drug-like properties of its glutarimide ligands such as thalidomide **1A**, pomalidomide **1B**, and lenalidomide **1C** (Figure 1).[5,8–12] These glutarimides were first applied to the development of PROTACs for targeted protein degradation in 2015.[13,14] The first two PROTACs progressed into clinical trials (ARV-110 and ARV-471) both used glutarimide CRBN ligands. However, glutarimides are used as a racemic mixture in almost all reported PROTACs because the two enantiomers can undergo rapid and spontaneous racemization *in vitro* and *in vivo*. For example, the racemization half-life of thalidomide is ~2.0 h in human blood and ~5.0 h *in-vivo* in humans, respectively.[15] The binding affinity of the (*S*)-enantiomeric thalidomide to CRBN is at least 10-fold stronger than the corresponding (*R*)-enantiomer.[16,17] The DDB1-CRBN-thalidomide complex further confirms that only the (*S*)-enantiomer fits the binding pocket well. The glutarimide moiety is most critical for binding as three hydrogen bonds are formed between the imide motif and CRBN, whereas the phthalimide or the phthalimidine moiety is exposed to the solvent.[18]

The use of racemic glutarimide as the E3 ligase ligands in PROTACs complicates many aspects of the drug development process and is one of the significant barriers for the therapeutic applications of CRBN-recruiting PROTACs. For example, half of the PROTAC molecules that have poor degradation activity due to ~10-fold weaker binding affinity to CRBN can competitively inhibit the other half of the active portion, because they bear the same POI ligand that can bind to the protein target. In addition, according to the FDA

policy updated in 1992, more resources are needed to characterize the pharmacological properties of all isomers including enantiomers or diastereomers and their metabolites during the drug development process.[19] To date, various CRBN ligands have been reported by researchers from both industry and academia; some of these reports include attempts to solve the chirality issue.[20–24] For example, the racemization of deuterated thalidomide **1D**, where the hydrogen is replaced by a deuterium, was about five times slower than thalidomide.[25] If an all carbon quaternary center was to be introduced, no racemization would occur. However, when the Y substituent in **1** was replaced by a methyl group, the corresponding compound **1E** lost its activity.[26,27] In addition to racemization, stability of the glutarimides is another issue. One of the major breakthroughs for the development of CRBN ligands is the design of phenyl glutarimides (PGs) **1F** for PROTACs during our study.[28] Significantly higher stability was observed after the replacement of the phthalimide or phthalimidine motif in thalidomide, pomalidomide, and lenalidomide by a simple phenyl ring in the PGs. Herein, we report the development of achiral phenyl dihydrouracil (PDHU) **2** as the CRBN ligands for the development of non-racemic PROTACs. Although both PGs and dihydrouracils were described as CRBN ligands in several patents,[20] detailed structure-activity relationship (SAR) and properties of the ligands were not disclosed, which prevent their broad applications for the development of PROTACs.

We began our investigation by examining the conformations of simple glutarimide and dihydrouracil (Figure 1) by extracting the relevant X-ray structures 4CI1[18] and 1R2Z[29] from Protein Data Bank. Glutarimide has a half-chair conformation, where five atoms in the imide ring are in the same plane. The remaining methylene group in the ring and the “G” substituent are out of the plane. In contrast, dihydrouracil is much flatter. The G-substituent on the nitrogen is in the same plane as the imide, while the carbonyl group pointed by the arrow and its adjacent methylene group are twisted out of the plane slightly. Before our study, it is not clear how the different orientation of G group and the twisted imide group will impact the binding of PDHU with the CRBN protein complex.

Results and Discussion

The parent PDHU **2** was prepared and its binding with the CRBN-DDB1 complex was compared with positive control lenalidomide **1C** using a known fluorescence polarization (FP) assay.[18] Lenalidomide was used as the positive control for comparison with PDHUs analogues and 84% of fluorescence probe was displaced by 1 μM of lenalidomide. All analogs were tested at a single concentration of 1 μM three times. As shown in Scheme 1, displacement observed for parent compound **2** was only around 20%, which is much worse than the 84% observed for lenalidomide positive control. This is not surprising based on the conformational analysis as discussed before. To improve the binding affinity, a series of disubstituted PDHUs were prepared. Various substituents were installed at the *ortho*, *meta*, and *para* positions of the phenyl group in PDHUs systematically and compared with the parent compound **2** for relative binding affinity. Interestingly, analogue **3A** with an *ortho* hydroxyl substituent almost completely lost the binding, while analogues **4A** and **5A** with a *meta* and *para* OH enhanced the binding to 57% and 38%, respectively. Methyl, ethyl and chloro substituents on the *ortho*-position (**3B**, **3D**, **3E**) improved the binding to 35%,

29% and 36% from the original 20% for the parent compound **2**. Compound **3C** with a methoxy substituent on the *ortho*-position decreased the binding, while placing the MeO on the *meta*-position (**4C**) improved the binding to 33%. Compounds **4F** and **4K** bearing longer substituents on the *meta*-position further improved the binding to 56% and 44%, respectively. Substituents on the *para*-positions were also tolerated, though they did not improve the binding as much as those on the *meta*-positions as shown in **5A** and **5K**.

Based on the structure-activity relationship (SAR) of the disubstituted PDHUs, we designed the second series of trisubstituted PDHUs. Considering the binding affinity observed for disubstituted PDHUs, ligand efficiency, metabolic stability and magic methyl effect,[30,31] *ortho* methyl was selected to explore its synergetic effect of binding improvement with the third substituent. Various 1,2,3-, 1,2,5- and 1,2,4-trisubstituted PDHUs were designed, synthesized, and compared with the lenalidomide positive control and compound **3B** with an *ortho* methyl substituent. We prepared more compounds with *meta*-substituents on the phenyl group of PDHUs since our results from the disubstituted PDHUs indicated that *meta*-substituents improved the binding more than the *para*-substituents. Among different groups, substituent **A** and **F** had the strongest synergetic effect. For example, the binding of **6F** and **7A** were improved to 78% and 81%, respectively. Most other trisubstituted PDHUs also showed better binding affinity than **3B**.

It is easiest to install linkers to the phenyl group on PDHUs bearing building blocks **F** and **K** for the development of PROTACs. We hypothesize that the *t*Bu group in these two building blocks can be replaced by various linkers for the development of non-racemic PROTACs that can recruit CRBN. With these in mind, we next measured the K_ds for lenalidomide **1C**, parent PDHU **2**, mono substituted PDHU **3B**, disubstituted PDHU **4F**, and trisubstituted PDUs **6F** and **6K** for further comparison (Figure 2). The K_d (0.17 μM) we observed in the FP assay for lenalidomide **1C** is very close to what was reported in the literature (K_d = 0.18 μM).[18] Parent PDHU **2** is 18 times weaker than lenalidomide **1C**. The installation of an *ortho*-Me in **3B** increased the affinity about 2.5 times. We were pleased to find that 1,2,3-Trisubstituted PDHU **6F** has a comparable K_d to lenalidomide. The difference between **6F** and **4F** confirms that the *ortho*- and *meta*-substituents in **6F** both contributed to the binding. Interestingly, the meta-substituent in PDHU **6K** does not further increase the binding compared to **3B**. We then prepared compounds **9** and **10** by replacing the *t*Bu with an amide functional group to confirm this observation. Similar K_ds were observed for compounds **6K**, **9** and **10**. We also extended the propargyl amide linker in **6F** to homopropargyl amide in **11**. Surprisingly, the affinity dropped three-fold in this case.

To establish a binding mode of the achiral ligands and rationalize the observed binding affinity trends, structural modeling was performed for representative structure **6F** based on docking followed by Molecular Dynamics (MD) refinement (Figure 3). The refinement allows both the ligand and protein to fully relax since ligand-induced changes may occur on protein side chains. Additionally, ligand binding stabilities can be observed during the refinement process, including filtering out false positive poses. The MD refinement procedure is similar to our previous method used for PROTAC modeling.[32] From these results, we observed that the carbamate carbonyl oxygen of **6F** form an H-bond with

neighboring Histidine 353. The phenyl, 2-methyl, 3-alkyne group and Boc t-butyl all form hydrophobic contacts with the protein. When the rigid alkyne is removed for **6K**, **9** and **10**, the direct hydrophobic contacts will be diminished and the H-bond will be disturbed. Compound **4F** being slightly weaker than **6F** is attributed to less hydrophobic space filling lacking the 2-methyl. Compound **11** with a rigid alkyne linker is expected to also form good contacts, but the extended linker length disturbs the H-bond with the carbonyl oxygen. Detailed procedures of the modeling and more images are provided in the SI.

We then further evaluated the stability of selected compounds (**6F** and **9–11**) in human liver microsomes (hLM), human plasma (hP) and buffer with different pHs (Table 1). Both compounds **6F** and **9–11** showed comparable stability to lenalidomide in hLM. In terms of stability in hP, only 62% of lenalidomide remained after 4h of incubation. In contrast, 97% of **6F** and over 80% of **9–11** remained under the same conditions. Under acidic conditions (pH=1.0), all compounds are very stable. However, under neutral conditions that mimic the physiological environment (pH=7.4 buffer), only 39% of lenalidomide was remained after 24 h of incubation at 37°C, while the hydrolysis of 1,2,3-trisubstituted PDHUs **6F** and **9–11** was not detected. PDHUs **6F** and **9–11** are much more stable than lenalidomide at slightly basic conditions (e.g. pH=8.8). Other than racemization, the ring opening of glutarimides by hydrolysis is a liability of CRBN-recruiting PROTACs.[33,34] Our results showed that the dihydrouracil motif has much higher stability and is less prone to hydrolysis. Based on the above data, we can conclude that the achiral CRBN ligands with 1,2,3-trisubstituted PDHUs such as **6F** can have similar binding affinity and much better stability profiles compared to lenalidomide.

It is well known that the binding of thalidomide, lenalidomide, pomalidomide, their analogues or certain PROTACs bearing the glutarimide motif to CRBN can induce the degradation of neo-substrates, such as IKZF1, IKZF3 and GSPT1.[1–5] The neo-substrate degradation activity can be changed by modifying the structure of CRBN ligand, the linking site, the property of the linker, or even the ligand of the POI in PROTACs. We next tested compounds **6F** and **9-11** in MV4;11 cells at two different concentrations (10 and 1 μM) for the degradation of IKZF1, IKZF3 and GSPT1. Western blot analysis indicated that these four compounds did not induce the degradation of IKZF1, IKZF3 or GSPT1 (Figure 4A–4C). Although this is encouraging, the selectivity of specific PROTACs bearing the achiral PDHU ligand should be examined thoroughly for the development of any therapeutics as the selectivity depends on the entire structure of the PROTAC.

The discovery of the achiral CRBN ligands provides an opportunity to develop various stereochemically well defined PROTACs that can recruit CRBN. To demonstrate the utility of these new CRBN ligands, (e.g., **6F** and **9–11**), we attached JQ1, a well-known ligand for BRD4, to the 1,2,3-trisubstituted PDHU and prepared potential BRD4 degraders **12A–12C**, **13** and **14** bearing several different linkers (Figure 5). These compounds were then tested in four different cell lines at two different concentrations (1.0 and 0.1 μM) for the degradation of BRD4. Western blot analysis indicated that compounds **12B**, **13** and **14** could induce the degradation of BRD4 protein in all four cell lines. Compound **12C** showed obviously BRD4 degradation activity in MV4;11 and LNCAP, however, **12A** bearing the shortest linker did not display activity in all four cell lines (Figure 6A). While compounds

12B, **13** and **14** displayed the most potent activity, compound **13** appeared to be slightly more potent. Our results indicated that the degradation efficiency was related to multiple parameters such as the length and type of linkers, in addition to the binding affinity of the achiral ligand to CRBN. Compound **13** was then selected for further characterization. We first studied the time course and dose response of degrader **13** (Figure 6B–E). Degradation of BRD4 occurred as early as 1 h post-treatment (Figure 6B). Degrader **13** also induced significant degradation of BRD4 at pM concentrations in MV4;11 cells with a DC_{50} of 22 pM and D_{max} of 97% (Figure 6C/D). We also verified the degradation effect of degrader **13** in a Flp-In™-293 cell line that stably expresses e-GFP-tagged BRD4 bromodomain (BD1) fusion and a non-targeted mCherry endogenous control (Figure 6E).[35] In the Flp-In™-293 cells, a DC_{50} of 34 nM and a D_{max} of 75% at 10 μM was observed. Interestingly, no obvious "Hook effect"[36] was observed with up to 10 μM for degrader **13**. The degrader was successful in inducing caspase 3 cleavage, a biomarker for cell apoptosis, at 10 nM to 10 μM concentrations.

We next verified the mechanism of action of degrader **13** (Figure 6G–H). Pretreatment of the cells with POI ligand JQ1, achiral CRBN ligand **9**, proteasome inhibitor MG132, and neddylation inhibitor MLN4924[37] abolished the BRD4 degradation induced by **13**, suggesting that the degradation involves the engagement of BRD4, CRBN, proteasome, and Cullin-RING E3 ligase complex. We also prepared negative control **13NT**, which has an additional methyl group on the imide motif that prevents the binding to CRBN.[18] As expected, no degradation activity of BRD4 was observed for **13NT** in MV4;11 cells at several different concentrations, further confirming the involvement of CRBN (Figure 6H). Finally, side-by-side comparison of degrader **13** with dBET1 was performed in MV4;11 cells. Degrader **13** showed more potent BRD4 degradation activity than dBET1 (Figure 6I).

We next investigated the functional outcomes of degrader **13** bearing an achiral CRBN ligand including cell proliferation, cell cycle arrest, and cell apoptosis (Figure 7). First, MV4;11 cells were treated by BRD4 degraders **13**, POI ligand (+)-JQ1, CRBN ligand **9**, and compound **13NT** for 72 h. As expected, compound **13** showed the most potent anti-proliferation activity with an IC_{50} value around 1.1 nM (Figure 7A). POI ligand (+)-JQ1 showed weaker anti-proliferation activity than **13**, but higher activity than compound **13NT**, which has a very similar structure to **13** but without CRBN recruiting ability. Compound **9**, which has the entire CRBN ligand and most parts of the linker, did not show any anti-proliferation activity at up to 100 μM. All these trends are expected and consistent with their mechanism of action. BRD4 degraders **13** could also induce G1 phase arrest, decrease the cell population in S phase, (Figure 7B) and induced cell apoptosis in a dose-dependent manner (Figure 7C and 7D) in MV4;11 cells.

Synthesis

Achiral CRBN ligands and BRD4 PROTACs were synthesized as shown in scheme 2. Various substituted PDHUs S2 can be prepared from the corresponding anilines S1 by adapting literature procedures through conjugate addition followed by cyclization (eq 1).[38] More substituents can be introduced to the phenyl group of PDHUs by Sonogashira coupling (eq 2), alkylation (eq 3 and eq 6), Suzuki cross coupling (eq 4), or Heck cross-coupling (eq

5). Further manipulations such as reduction (eq 7) and de-protection of Boc group followed by amide formation can afford ligands **6G, 9**, and **11**, respectively.

BRD4 PROTACs bearing achiral CRBN ligands were synthesized as shown in scheme 3. Removal of the Boc protecting group in intermediate **S4** followed by amide coupling with JQ1 afforded PROTACs **12A-C**. Removal of the *t*Bu protecting group in intermediate **S5** followed by coupling with a linker, de-protection, and reaction with JQ1 yielded PROTACs **13**, **14** and the negative control **13NT**.

Conclusion

Racemization has been a long-standing issue for most CRBN recruiting PROTACs. Due to the racemization between active and inactive enantiomers, CRBN-based PROTACs face not only the issue of half of the PROTAC molecules possessing low E3-ligase binding activity, but also the issue of these low-potency molecules acting as inhibitors to compete with the other half of active PROTACs at the POI binding site. In addition, the half of PROTACs with low E3 ligase binding activity also produce various metabolites that require additional characterization and careful monitoring. These issues significantly complicate the development and manufacturing of PROTACs as therapeutics. Although many molecular glues and PROTACs bearing a racemic CRBN ligand have successfully entered into clinic trials or gained approval, more resources are required to characterize the pharmacological properties of the inactive isomeric compounds according to FDA policy.[19] We have developed various substituted PDHUs as a novel class of achiral CRBN ligands and discovered interesting SAR. Although there is only one atom change from PGs to PDHUs, the conformation of dihydrouracil ring in PDHU becomes much flatter than the glutarimide ring in PGs, which results in much weaker binding affinity of the parent PDHU than the parent PG. Through the SAR study of a series of disubstituted and trisubstituted PDHUs, we found that substituted achiral PDHUs could achieve similar binding affinities to lenalidomide, but with much higher stability. Structural modeling studies revealed the additional interactions one can pick up by adding various substituents to the phenyl group, which provides a path for further optimization in the future. Finally, five 1,2,3-trisubstituted PDHU-based BRD4 PROTACs were designed and synthesized. Their remarkable BRD4 degradation activities were verified in multiple cell lines and two orthogonal methods – Western blot analysis of the endogenous BRD4 and fluorescent quantification of $BRD4_{BD1}$-e-GFP fusion protein, demonstrating that substituted PDHUs can be used for the development of non-racemic CRBN recruiting PROTACs. We anticipate that the readily accessible substituted PDHUs such as **6F** and **9** will be widely used for the development of various PROTACs.

Experimental section

Cell Culture

Three human leukemia cell lines (MV4;11, RS4;11, MOLT4) and one prostate cancer cell line (LNCAP) were obtained from ATCC, expanded, and frozen down in cryogenic vials. Cells were thawed and used within 20 passages in the experiments. All cells were cultured in RPMI1640 media (Corning) supplemented with 10% fetal bovine serum (FBS)

and 1% Penicillin and Streptomycin in a CO_2 incubator (37 °C, with humidified 5% CO_2 atmosphere).

AlamarBlue Cell Viability

Cells were seeded in a 96-well plate at a density of 5000–10000 cells in 100 μl media per well and treated with DMSO control or test compounds at indicated doses. After incubated in CO_2 incubator for 72 hours, cells were treated with 10 μL AlamarBlue solution (440 mM)). Fluorescence was measured in a plate reader with an excitation wavelength at 530–560 nm and emission wavelength at 590 nm. The fluorescence was normalized to the DMSO-treated cells, and the IC_{50} was calculated using GraphPad Prism 9 software.

Western Blot Assay

Cells were treated with test compounds at indicated doses, incubated for the indicated time, and then lysed in RIPA plus protease inhibitors. The protein concentration was determined by the BCA assay. Equivalent amounts of protein were loaded and separated in 7.5% SDS-PAGE gels and transferred to PVDF membranes. Membranes were blocked in 5% BSA/TBST solution and then incubated with the appropriate primary antibodies diluted in 5% BSA/TBST in a cold room overnight. After being washed, the membranes were incubated with the appropriate HRP-conjugated secondary antibodies in 2% BSA/TBST for one h at room temperature and then washed again. Bound antibodies were visualized using ECL assay (Bio-Rad), and images were captured using the ChemidocTMMP imaging system (Bio-Rad). All antibodies were purchased from Cell signaling Technology, including Anti-Brd4 (CS#13440), anti-Caspase 3 (CS#9662), Anti-β-Actin (CS#3700), and HRP-conjugated anti-mouse IgG (CS#7076) and HRP-conjugated anti-rabbit IgG (CS#7074).

Flow Cytometry

Cell apoptosis and cell cycle were detected by Attune Flow cytometer (Thermo Fisher). Cells were seeded in a 6-well plate and treated with the indicated concentrations of compounds for 48 h. For samples for cell apoptosis detection, cells were harvested and incubated in Annexin V-FITC and PI reagents each for 15 minutes (Annexin V-FITC apoptosis detection kit, Invitrogen). For the samples for cell cycle detection, cells were fixed in 70% cold ethanol overnight and stained with PI (500μg/ml) for 15 minutes. Flow data were analyzed using Flowjo software.

Cellular Degradation in Flp-In™-293 Cell

BRD4BD1 mammalian pcDNA5/FRT Vector (Ampicillin and Hygromycin B resistant) with MCS-eGFP-P2A-mCherry was obtained from Fischer's lab.[35] Stable cell lines expressing eGFP-protein fusion and mCherry reporter were generated using the Flp-In 293 system according to the manual from the vendor (Thermo Fisher). Plasmid (0.4 μg) and pOG44 (3.6 μg) DNA were pre-incubated in Opti-MEM media with 12 μL FuGene HD and added to Flp-In 293 cells (REF R75007, ThermoFisher) containing DMEM media per well in a 6-well plate format. Cells were propagated after 48 h and transferred into a 10 cm^2 plate in DMEM media containing 50 μg/ml of Hygromycin B as a selection marker. Positive

colonies were split into a 60 mm dish until confluent and subsequently propagated. eGFP and mCherry signal were confirmed by flow cytometry for assay validation.

Cells were seeded at 5×10^5 per well in 24-well plates one day prior to compound treatment. Titrated compounds were incubated with cells for 24 h followed by detachment and resuspension in PBS with 2% FBS, filtration, and transferred into 5 mL polystyrene tubes for analysis by flow cytometry (Attune, Thermo Fisher). Signal from at least 50,000 events per well was acquired, and the eGFP and mCherry fluorescence monitored. Data were analyzed using FlowJo (FlowJo, LCC). Forward and side scatter outliers were removed by gating. The eGFP signal abundance relative to mCherry was then quantified as a ten-fold amplified ratio using the formula: 10 × eGFP/mCherry. The median fluorescence intensity (MFI) was calculated for eGFP and mCherry for each sample and normalized to the DMSO ratio.

General Information in Synthetic Chemistry

All reactions were conducted under a positive pressure of dry argon in a glassware that had been oven-dried prior to use. Anhydrous solutions of reaction mixtures were transferred via an oven-dried syringe or cannula. All solvents were dried prior to use unless noted otherwise. Thin-layer chromatography (TLC) was performed using precoated silica gel plates. Flash column chromatography was performed with the silica gel. ^{1}H and ^{13}C nuclear magnetic resonance (NMR) spectra were recorded on Bruker 400, 500, 600 MHz and Varian 500 MHz spectrometers. ^{1}H NMR spectra were reported in parts per million (ppm) referenced to 7.26 ppm of $CDCl_3$ or referenced to the center line of a septet at 2.50 ppm of DMSO-d_6. Signal splitting patterns were described as singlet (s), doublet (d), triplet (t), quartet (q), quintet (quint), or multiplet (m), with coupling constants (J) in hertz. High-resolution mass spectra (HRMS) were performed on an electron spray injection (ESI) TOF mass spectrometer. The liquid chromatography–mass spectrometry (LC–MS) analysis of final products was processed on an Agilent 1290 Infinity II LC system using a Poroshell 120 EC-C18 column (5 cm × 2.1 mm, 1.9 μm) for chromatographic separation. Purity is >95% as determined by HPLC for all final compounds tested for biological activities.

General procedure for preparation of Phenyl Dihydrouracils—In a 250 mL flask with a magnetic stirring bar, a solution of known 4-hydroxyaniline (4.37 g, 40.0 mmol) in toluene (50 mL, 0.8 M) was added acrylic acid (3.57 mL, 52.0 mmol). The reaction mixture stirred at 110 °C until the staring material disappeared as indicated by TLC, then the toluene was removed by rotavapor. Acetic acid (60 mL) and urea (7.20 g, 120.0 mmol) was then added to the flask and heated to 120 °C for 16 hours. Most of the acetic acid was removed by rotavapor. The residue was then dissolved in water (100 mL) and extracted by ethyl acetate (3×100 mL). The organic layers were combined, dried over Na_2SO_4, and concentrated under reduced pressure. The solid residue was suspended in ethyl acetate (10 mL) and stirred for 2 hours. The slurry was filtrated and the solid was wash by ethyl acetate (2×5 mL). Compound **5A** (2.75 g, yield 33%) was obtain as solid.

General procedure for preparation of 4F, 6F and 7F by Sonogashira Couplings —A 25 mL flask was charge with magnetic stirring bar, compound **4** (316 mg, 1.0 mmol),

N-Boc-propargylamine (466 mg, 3.0 mmol), $Pd(PPh_3)_2Cl_2$ (35 mg, 0.05 mmol) and CuI (10 mg, 0.05 mmol), evacuated and backfilled with argon. Dimethylformamide (DMF) (2.5 mL) and Triethylamine (NEt_3) (2.5 mL) were successively added by syringe. The reaction mixture stirred at room temperature until the staring material compound **4** disappeared as indicated by TLC. The mixture was partitioned between ethyl acetate and saturated solution of sodium bicarbonate, the organic layer was washed with brine, dried over Na_2SO_4, and concentrated in vacuum. The residue was purified by column chromatography on silica to provide **4F** (260 mg, yield 75%) as white solid.

General procedure for preparation of 4H, 6H, 7H and 8H—A 35 mL pressure tube was charge with magnetic stirring bar, compound **4A** (412 mg, 2.0 mmol). Next 1-Boc-4-bromopiperidine (1585 mg, 6.0 mmol), K_2CO_3 (910 mg, 6.6 mmol) and acetonitrile (10 mL) was added. Then the reaction mixture was stirred at 110 °C for 18 hours. The mixture was partitioned between ethyl acetate and water, the organic layer was washed with brine, dried over Na_2SO_4, and concentrated in vacuum. The residue was purified by column chromatography on silica to provide **4H** (241 mg, yield 31%) as white solid.

General procedure for preparation of 6I and 7I by Suzuki Couplings—A 25 mL flask was charge with magnetic stirring bar, compound **7** (330 mg, 1.0 mmol), 4-Formylphenylboronic acid (300 mg, 2.0 mmol), $Pd(dppf)Cl_2$ (36 mg, 0.05 mmol) and KOAc (295 mg, 3.0 mmol), evacuated and backfilled with argon. Dimethyl sulfoxide (DMSO) (5.0 mL) was added by syringe. The reaction mixture stirred at 90 °C until the staring material compound **7** disappeared as indicated by TLC. The mixture was partitioned between ethyl acetate and saturated solution of sodium bicarbonate, the organic layer was washed with brine, dried over Na_2SO_4, and concentrated in vacuum. The residue was purified by column chromatography on silica to provide **7I** (133 mg, yield 43%) as white solid.

General procedure for preparation of 6J, 7J and 8J—A 35 mL pressure tube was charge with magnetic stirring bar, compound **6A** (440 mg, 2.0 mmol). Next 4-(Chloromethyl)benzaldehyde (310 mg, 2.0 mmol), K_2CO_3 (608 mg, 4.4 mmol) and acetonitrile (10 mL) was added. Then the reaction mixture was stirred at 80 °C until the staring material compound **7** disappeared as indicated by TLC. The mixture was partitioned between ethyl acetate and water, the organic layer was washed with brine, dried over Na_2SO_4, and concentrated in vacuum. The residue was purified by column chromatography on silica to provide **6J** (162 mg, yield 24%) as white solid.

General procedure for preparation of 4K, 5K, 6K, 7K and 8K—A 35 mL pressure tube was charge with magnetic stirring bar, compound **4A** (620 mg, 3.0 mmol). Next tert-Butyl bromoacetate (0.465 mL, 3.15 mmol), K_2CO_3 (910 mg, 6.6 mmol) and acetonitrile (15 mL) was added. Then the reaction mixture was stirred at 80 °C until the staring material compound **7** disappeared as indicated by TLC. The mixture was partitioned between ethyl acetate and water, the organic layer was washed with brine, dried over Na_2SO_4, and concentrated in vacuum. The residue was purified by column chromatography on silica to provide **4K** (662 mg, yield 69%) as white solid.

General procedure for preparation of 6M and 7M by Heck Reaction—A 25 mL flask was charge with magnetic stirring bar, compound **7** (165 mg, 0.5 mmol), $Pd(OAc)_2$ (11 mg, 0.05 mmol) and P(*o*-tol)$_3$ (38 mg, 0.12 mmol), evacuated and backfilled with argon. Dimethylformamide (DMF) (3.0 mL), Triethylamine (NEt_3) (0.21 mL, 1.5 mmol) and tert-Butyl acrylate (0.22 mL, 1.5 mmol) were successively added by syringe. The reaction mixture stirred at 100 °C until the staring material compound **7** disappeared as indicated by TLC. The mixture was partitioned between ethyl acetate and saturated solution of sodium bicarbonate, the organic layer was washed with brine, dried over Na_2SO_4, and concentrated in vacuum. The residue was purified by column chromatography on silica to provide **7M** (101 mg, yield 61%) as white solid.

General procedure for preparation of 6G, 7G, 6L and 7L—A 20 mL vial was charge with magnetic stirring bar and compound **6F** (50 mg, 0.14 mmol). Next methanol (3.0 mL) and palladium on carbon (10 wt. %) (20 mg) was added. A hydrogen balloon was connected with the reaction mixture through a needle. The reaction mixture stirred at room temperature until the staring material compound **6F** disappeared as indicated by TLC. The mixture was filtrated by celite and wash by methanol (3×5 mL). The methanol solution was concentrated in vacuum to provide 6G (48 mg, yield 95%) as white solid.

General procedure for preparation of 9 and 10.—A 20 mL vial was charge with magnetic stirring bar and compound **6K** (67 mg, 0.2 mmol). Next dichloromethane (DCM) (0.5 mL) and trifluoroacetic acid (TFA) (0.75 mL) was added. The reaction mixture stirred at room temperature until the staring material compound **6K** disappeared as indicated by TLC. The mixture was concentrated in vacuum to provide white solid. In the same vial, DMF (1.0 mL), piperidine (0.02 mL, 0.2 mmol), triethylamine (0.112 mL, 0.8 mmol) and 1-[Bis(dimethylamino)methylene]-1H-1,2,3-triazolo[4,5-b]pyridinium 3-oxide hexafluorophosphate (HATU) (91 mg, 0.24 mmol) were successively added. The reaction mixture stirred at room temperature until the staring material disappeared as indicated by TLC. The mixture was partitioned between ethyl acetate and saturated solution of sodium bicarbonate, the organic layer was washed with brine, dried over Na_2SO_4, and concentrated in vacuum. The residue was purified by column chromatography on silica to provide **9** (42 mg, yield 61%) as white solid.

Procedure for preparation of 11.—A 20 mL vial was charge with magnetic stirring bar and tert-butyl (4-(3-(2,4-dioxotetrahydropyrimidin-1(2H)-yl)-2-methylphenyl)but-3-yn-1-yl)carbamate (74 mg, 0.2 mmol). Next, HCl/dioxane (1.0 mL, 4M) was added by syringe. The mixture was stirred at room temperature for half-hour, TLC indicated that the reaction was completed. The reaction mixture was concentrated under high vacuum at room temperature to provide solid. The solid was dissolved by DMF (1.0 mL) in the same vial, triethylamine (0.136 mL, 0.98 mmol) and acetic anhydride (0.021 mL, 0.22 mmol) were successively added. The reaction mixture stirred at room temperature until the staring material disappeared as indicated by TLC. The mixture was partitioned between ethyl acetate and saturated solution of sodium bicarbonate, the organic layer was washed with brine, dried over Na_2SO_4, and concentrated in vacuum. The residue was purified by column chromatography on silica to provide **11** (30 mg, yield 48%) as white solid.

General procedure for preparation of 12A, 12B and 12C.—A 20 mL vial was charge with magnetic stirring bar and **6F** (54 mg, 0.15 mmol). Next, HCl/dioxane (1.0 mL, 4M) was added by syringe. The mixture was stirred at room temperature for half-hour, TLC indicated that the reaction was completed. The reaction mixture was concentrated under high vacuum at room temperature to provide solid. The solid was dissolved by DMF (1.0 mL) in the same vial, *N*,*N*-diisopropylethylamine (DIPEA) (0.107 mL, 0.6 mmol), JQ-1 (carboxylic acid) (Purchase from MedChemExpress Part NO.: HY-78695) (60 mg, 0.15 mmol) and HATU (63 mg, 0.165 mmol) were successively added. The mixture was stirred at room temperature for half-hour, TLC indicated that the reaction was completed. The mixture was partitioned between ethyl acetate and saturated solution of sodium bicarbonate, the organic layer was washed with brine, dried over Na_2SO_4, and concentrated in vacuum. The residue was purified by column chromatography on silica to provide **12A** (83 mg, yield 86%) as white solid.

Procedure for preparation of 6K-Me tert-butyl 2-(2-methyl-3-(3-methyl-2,4-dioxotetrahydropyrimidin-1(2H)-yl)phenoxy)acetate—A 20 mL vial was charge with magnetic stirring bar, compound **6K** (100 mg, 0.3 mmol) and Cs_2CO_3 (108 mg, 0.33 mmol). Next, DMF (1.0 mL) and iodomethane (MeI) (0.023 mL, 0.36 mmol) was added by syringe. The mixture was stirred at room temperature until the staring material **6K** disappeared as indicated by TLC. The mixture was partitioned between ethyl acetate and saturated solution of sodium bicarbonate, the organic layer was washed with brine, dried over Na_2SO_4, and concentrated in vacuum, the residue was directly used for next step reaction without further purification.

General procedure for preparation of 13, 13NT and 14—A 20 mL vial was charge with magnetic stirring bar and **6K** (51 mg, 0.15 mmol). Next DCM (0.5 mL) and TFA (0.75 mL) was added. The reaction mixture stirred at room temperature until the staring material compound **6K** disappeared as indicated by TLC. The mixture was concentrated in vacuum to provide white solid. In the same vial, DMF (0.5 mL), 4-(*N*-Boc-amino)piperidine (30 mg, 0.15 mmol), DIPEA (0.107 mL, 0.6 mmol) and HATU (63 mg, 0.165 mmol) were successively added. The reaction mixture stirred at room temperature until the staring material disappeared as indicated by TLC. The mixture was partitioned between ethyl acetate and saturated solution of sodium carbonate, the organic layer was washed with brine, dried over Na_2SO_4, and concentrated in vacuum. The residue was treated by DCM (0.75 mL) and TFA (0.75 mL) at room temperature for half-hour, TLC indicated that the reaction was completed. The mixture was concentrated in high vacuum, in the same vial, DIPEA (0.107 mL, 0.6 mmol), JQ-1 (carboxylic acid) (60 mg, 0.15 mmol) and HATU (63 mg, 0.165 mmol) were successively added. The mixture was stirred at room temperature for half-hour, TLC indicated that the reaction was completed. The mixture was partitioned between ethyl acetate and saturated solution of sodium bicarbonate, the organic layer was washed with brine, dried over Na_2SO_4, and concentrated in vacuum. The residue was purified by column chromatography on silica to provide **13** (85 mg, yield 76%) as white solid.

Compound Characterization Data

1-phenyldihydropyrimidine-2,4(1H,3H)-dione (2)—^{1}H NMR (400 MHz, DMSO-d_6) δ 10.36 (s, 1H), 7.43 – 7.35 (m, 2H), 7.39 – 7.29 (m, 2H), 7.27 – 7.19 (m, 1H), 3.79 (t, J = 6.7 Hz, 2H), 2.70 (t, J = 6.7 Hz, 2H). ^{13}C NMR (101 MHz, DMSO-d_6) δ 170.6, 152.1, 142.1, 128.6, 125.8, 125.3, 44.5, 31.1. HPLC purity: 97.8%.

1-(2-hydroxyphenyl)dihydropyrimidine-2,4(1H,3H)-dione (3A)—^{1}H NMR (400 MHz, DMSO-d_6) δ 7.45 (s, 1H), 7.34 – 7.26 (m, 2H), 7.24 – 7.17 (m, 1H), 7.15 – 7.07 (m, 1H), 6.91 (s, 1H), 4.00 (t, J = 6.9 Hz, 2H), 2.53 (t, J = 6.9 Hz, 3H). ^{13}C NMR (101 MHz, DMSO-d_6) δ = 171.6, 153.6, 141.9, 131.0, 123.8, 122.1, 109.6, 109.5, 38.5, 33.1. HRMS (ESI/[M+H]$^+$) Calcd for [$C_{10}H_{10}N_2O_3$+H]$^+$: 207.0764, found: 207.0765. HPLC purity: 98.6%.

1-(o-tolyl)dihydropyrimidine-2,4(1H,3H)-dione (3B)—^{1}H NMR (400 MHz, DMSO-d_6) δ 10.33 (s, 1H), 7.33 – 7.18 (m, 4H), 3.82 – 3.71 (m, 1H), 3.55 – 3.45 (m, 1H), 2.86 – 2.60 (m, 2H), 2.19 (s, 3H). ^{13}C NMR (101 MHz, DMSO-d_6) δ = 170.8, 151.7, 140.9, 135.5, 130.6, 127.4, 127.2, 126.8, 44.6, 31.1, 17.5. HRMS (ESI/[M+H]$^+$) Calcd for [$C_{11}H_{12}N_2O_2$+H]$^+$: 205.0972, found: 205.0973. HPLC purity: 97.5%.

1-(2-methoxyphenyl)dihydropyrimidine-2,4(1H,3H)-dione (3C)—^{1}H NMR (400 MHz, DMSO-d_6) δ 10.29 (s, 1H), 7.36 – 7.28 (m, 1H), 7.27 – 7.21 (m, 1H), 7.14 – 7.07 (m, 1H), 7.01 – 6.92 (m, 1H), 3.80 (s, 3H), 3.57 (t, J = 6.7 Hz, 2H), 2.67 (t, J = 6.6 Hz, 2H). ^{13}C NMR (101 MHz, DMSO-d_6) δ = 170.8, 154.8, 152.1, 130.1, 129.2, 128.8, 120.5, 112.4, 55.7, 44.5, 31.1. HRMS (ESI/[M+H]$^+$) Calcd for [$C_{11}H_{12}N_2O_3$+H]$^+$: 221.0921, found: 221.0924. HPLC purity: 98.2%.

1-(2-ethylphenyl)dihydropyrimidine-2,4(1H,3H)-dione (3D)—^{1}H NMR (400 MHz, DMSO-d_6) δ 10.34 (s, 1H), 7.36 – 7.23 (m, 4H), 3.84 – 3.72 (m, 1H), 3.52 – 3.41 (m, 1H), 2.83 – 2.62 (m, 2H), 2.54 (tt, J = 7.6, 3.8 Hz, 2H), 1.15 (t, J = 7.6 Hz, 3H). ^{13}C NMR (101 MHz, DMSO-d_6) δ 170.7, 152.2, 141.2, 140.4, 128.8, 127.8, 127.6, 126.8, 45.0, 31.1, 23.5, 14.4. HRMS (ESI/[M+H]+) Calcd for [$C_{12}H_{14}N_2O_2$+H]$^+$: 219.1128, found: 219.1131. HPLC purity: 97.6%.

1-(2-chlorophenyl)dihydropyrimidine-2,4(1H,3H)-dione (3E)—^{1}H NMR (400 MHz, DMSO-d_6) δ 10.47 (s, 1H), 7.61 – 7.54 (m, 1H), 7.53 – 7.46 (m, 1H), 7.45 – 7.34 (m, 2H), 3.77 – 3.66 (m, 1H), 3.65 – 3.54 (m, 1H), 2.77 – 2.69 (m, 2H). ^{13}C NMR (101 MHz, DMSO-d_6) δ 170.6, 151.8, 139.0, 131.8, 130.1, 129.9, 129.3, 128.2, 44.3, 31.0. HRMS (ESI/[M+H]+) Calcd for [$C_{10}H_9ClN_2O_2$+H]$^+$: 225.0425, found: 225.0425. HPLC purity: 95.8%.

1-(3-iodophenyl)dihydropyrimidine-2,4(1H,3H)-dione (4)—^{1}H NMR (400 MHz, DMSO-d_6) δ 10.42 (s, 1H), 7.76 – 7.70 (m, 1H), 7.63 – 7.56 (m, 1H), 7.39 – 7.32 (m, 1H), 7.23 – 7.15 (m, 1H), 3.78 (t, J = 6.6 Hz, 2H), 2.69 (t, J = 6.6 Hz, 2H). ^{13}C NMR (101 MHz, DMSO-d_6) δ 170.6, 152.1, 143.3, 134.4, 133.9, 130.5, 124.7, 94.0, 44.4, 31.0.

1-(3-hydroxyphenyl)dihydropyrimidine-2,4(1H,3H)-dione (4A)—^{1}H NMR (400 MHz, DMSO-d_6) δ 10.31 (s, 1H), 9.54 (s, 1H), 7.20 – 7.12 (m, 1H), 6.76 – 6.69 (m, 2H), 6.67 – 6.60 (m, 1H), 3.73 (t, J = 6.6 Hz, 2H), 2.68 (t, J = 6.6 Hz, 2H). ^{13}C NMR (101 MHz, DMSO-d_6) δ 170.6, 157.5, 152.0, 143.1, 129.3, 115.6, 112.9, 112.6, 44.6, 31.1. HRMS (ESI/[M+H]+) Calcd for $[C_{10}H_{10}N_2O_3+H]^+$: 207.0764, found: 207.0764. HPLC purity: 95.4%.

1-(3-methoxyphenyl)dihydropyrimidine-2,4(1H,3H)-dione (4C)—^{1}H NMR (400 MHz, DMSO-d_6) δ 10.35 (s, 1H), 7.33 – 7.24 (m, 1H), 6.94 – 6.86 (m, 2H), 6.86 – 6.78 (m, 1H), 3.77 (t, J = 6.7 Hz, 2H), 3.75 (s, 3H), 2.69 (t, J = 6.7 Hz, 2H). ^{13}C NMR (101 MHz, DMSO-d_6) δ 170.6, 159.4, 152.1, 143.2, 129.3, 117.5, 111.4, 111.4, 55.2, 44.6, 31.1. HRMS (ESI/$[M+H]^+$) Calcd for $[C_{11}H_{12}N_2O_3+H]^+$: 221.0921, found: 221.0922. HPLC purity: 95.3%.

tert-butyl (3-(3-(2,4-dioxotetrahydropyrimidin-1(2H)-yl)phenyl)prop-2-yn-1-yl)carbamate (4F)—^{1}H NMR (400 MHz, DMSO-d_6) δ 10.41 (s, 1H), 7.49 – 7.32 (m, 4H), 7.29 – 7.22 (m, 1H), 3.98 (d, J = 5.8 Hz, 2H), 3.79 (t, J = 6.6 Hz, 2H), 2.70 (t, J = 6.6 Hz, 2H), 1.40 (s, 9H). ^{13}C NMR (101 MHz, DMSO-d_6) δ 170.6, 155.3, 152.1, 142.2, 129.0, 128.5, 128.0, 125.4, 122.6, 88.0, 80.9, 78.3, 44.3, 31.0, 30.1, 28.2. HRMS (ESI/$[M+Na]^+$) Calcd for $[C_{18}H_{21}N_3O_4+Na]^+$: 366.1424, found: 366.1420. HPLC purity: 98.9%.

tert-butyl 4-(3-(2,4-dioxotetrahydropyrimidin-1(2H)-yl)phenoxy)piperidine-1-carboxylate (4H)—^{1}H NMR (400 MHz, DMSO-d_6) δ 10.35 (s, 1H), 7.32 – 7.23 (m, 1H), 6.98 – 6.93 (m, 1H), 6.92 – 6.82 (m, 2H), 4.60 – 4.49 (m, 1H), 3.77 (t, J = 6.7 Hz, 2H), 3.70 – 3.60 (m, 2H), 3.24 – 3.14 (m, 2H), 2.69 (t, J = 6.7 Hz, 2H), 1.98 – 1.85 (m, 2H), 1.57 – 1.47 (m, 2H), 1.40 (s, 8H). ^{13}C NMR (101 MHz, DMSO-d_6) δ 170.6, 157.0, 153.9, 152.1, 143.3, 129.4, 117.7, 113.3, 113.2, 78.7, 71.9, 48.6, 44.6, 31.0, 30.3, 28.1. HRMS (ESI/$[M+H]^+$) Calcd for $[C_{20}H_{27}N_3O_5+H]^+$: 390.2023, found: 390.2022. HPLC purity: 95.6%.

tert-butyl 2-(3-(2,4-dioxotetrahydropyrimidin-1(2H)-yl)phenoxy)acetate (4K)—^{1}H NMR (400 MHz, DMSO-d_6) δ 10.36 (s, 1H), 7.34 – 7.24 (m, 1H), 6.97 – 6.88 (m, 2H), 6.81 – 6.73 (m, 1H), 4.65 (s, 2H), 3.76 (t, J = 6.6 Hz, 2H), 2.69 (t, J = 6.6 Hz, 2H), 1.43 (s, 9H). ^{13}C NMR (101 MHz, DMSO-d_6) δ 170.6, 167.7, 157.8, 152.0, 143.1, 129.3, 118.1, 112.1, 111.6, 81.4, 65.1, 44.6, 31.0, 27.7. HRMS (ESI/$[M+H]^+$) Calcd for $[C_{16}H_{20}N_2O_5+H]^+$: 321.1445, found: 321.1444. HPLC purity: 97.4%.

1-(4-hydroxyphenyl)dihydropyrimidine-2,4(1H,3H)-dione (5A)—^{1}H NMR (400 MHz, DMSO-d_6) δ 10.25 (s, 1H), 9.46 (s, 1H), 7.14 – 7.06 (m, 2H), 6.79 – 6.71 (m, 2H), 3.67 (t, J = 6.7 Hz, 2H), 2.67 (t, J = 6.7 Hz, 2H). ^{13}C NMR (101 MHz, DMSO-d_6) δ 170.7, 155.6, 152.3, 133.5, 127.0, 115.2, 45.1, 31.1. HRMS (ESI/[M+H]+) Calcd for $[C_{10}H_{10}N_2O_3+H]^+$: 207.0764, found: 207.0763. HPLC purity: 99.0%.

tert-butyl 2-(4-(2,4-dioxotetrahydropyrimidin-1(2H)-yl)phenoxy)acetate (5K)

^{1}H NMR (400 MHz, DMSO-d_6) δ 10.30 (s, 1H), 7.28 – 7.19 (m, 2H), 6.95 – 6.86 (m, 2H), 4.65 (s, 2H), 3.72 (t, J = 6.7 Hz, 2H), 2.69 (t, J = 6.7 Hz, 2H), 1.44 (s, 9H). ^{13}C NMR

(101 MHz, DMSO-d_6) δ 170.6, 167.8, 155.6, 152.3, 135.4, 126.8, 114.5, 81.4, 65.1, 44.9, 31.1, 27.7. HRMS (ESI/[M+H]$^+$) Calcd for [$C_{16}H_{20}N_2O_5$+H]$^+$: 321.1445, found: 321.1448. HPLC purity: 98.8%.

1-(3-iodo-2-methylphenyl)dihydropyrimidine-2,4(1H,3H)-dione (6)—^{1}H NMR (400 MHz, DMSO-d_6) δ 10.40 (s, 1H), 7.82 (dd, J = 7.9, 1.2 Hz, 1H), 7.33 (dd, J = 7.9, 1.2 Hz, 1H), 7.07 – 6.98 (m, 1H), 3.83 – 3.72 (m, 1H), 3.57 – 3.46 (m, 1H), 2.86 – 2.73 (m, 1H), 2.73 – 2.62 (m, 1H), 2.28 (s, 3H). ^{13}C NMR (101 MHz, DMSO-d_6) δ = 170.7, 151.8, 141.0, 138.8, 138.1, 128.6, 127.7, 102.2, 44.6, 31.0, 23.5.

1-(3-hydroxy-2-methylphenyl)dihydropyrimidine-2,4(1H,3H)-dione (6A)—^{1}H NMR (400 MHz, DMSO-d_6) δ 10.28 (s, 1H), 9.49 (s, 1H), 7.06 – 6.98 (m, 1H), 6.81 – 6.74 (m, 1H), 6.73 – 6.67 (m, 1H), 3.77 – 3.66 (m, 1H), 3.52 – 3.42 (m, 1H), 2.81 – 2.70 (m, 1H), 2.70 – 2.59 (m, 1H), 1.97 (s, 3H). ^{13}C NMR (101 MHz, DMSO-d_6) δ 170.8, 156.0, 151.7, 141.9, 126.3, 122.3, 117.6, 113.7, 44.7, 31.1, 10.7. HRMS (ESI/[M+H]$^+$) Calcd for [$C_{11}H_{12}N_2O_3$+H]$^+$: 221.0921, found: 221.0922. HPLC purity: 98.0%.

tert-butyl (3-(3-(2,4-dioxotetrahydropyrimidin-1(2H)-yl)-2-methylphenyl)prop-2-yn-1-yl)carbamate (6F)—^{1}H NMR (400 MHz, DMSO-d_6) δ 10.37 (s, 1H), 7.46 – 7.36 (m, 1H), 7.36 – 7.18 (m, 3H), 4.00 (d, J = 5.8 Hz, 2H), 3.85 – 3.69 (m, 1H), 3.58 – 3.44 (m, 1H), 2.87 – 2.58 (m, 2H), 2.24 (s, 3H), 1.40 (s, 9H). ^{13}C NMR (101 MHz, DMSO-d_6) δ 170.7, 155.4, 151.8, 141.3, 137.7, 130.7, 127.6, 126.7, 123.6, 91.9, 79.9, 78.2, 44.5, 31.1, 30.3, 28.2, 15.6. HRMS (ESI/[M+Na]$^+$) Calcd for [$C_{19}H_{23}N_3O_4$+Na]$^+$: 380.1581, found: 380.1575. HPLC purity: 98.6%.

tert-butyl (3-(3-(2,4-dioxotetrahydropyrimidin-1(2H)-yl)-2-methylphenyl)propyl)carbamate (6G)—^{1}H NMR (400 MHz, DMSO-d_6) δ 10.30 (s, 1H), 7.19 – 7.08 (m, 3H), 6.95 – 6.87 (m, 1H), 3.79 – 3.67 (m, 1H), 3.53 – 3.42 (m, 1H), 3.03 – 2.94 (m, 2H), 2.84 – 2.72 (m, 1H), 2.72 – 2.62 (m, 1H), 2.62 – 2.54 (m, 2H), 2.09 (s, 3H), 1.62 (p, J = 7.0 Hz, 2H), 1.38 (s, 9H). ^{13}C NMR (101 MHz, DMSO-d_6) δ 170.8, 155.7, 151.9, 141.4, 141.2, 133.6, 128.0, 126.2, 124.9, 77.4, 44.8, 31.1, 30.5, 30.1, 28.3, 13.2. HRMS (ESI/[M+H]$^+$) Calcd for [$C_{19}H_{27}N_3O_4$+H]$^+$: 362.2074, found: 362.2080. HPLC purity: 98.3%.

tert-butyl 4-(3-(2,4-dioxotetrahydropyrimidin-1(2H)-yl)-2-methylphenoxy)piperidine-1-carboxylate (6H)—^{1}H NMR (400 MHz, DMSO-d_6) δ ^{1}H NMR (400 MHz, DMSO) δ 10.32 (s, 1H), 7.23 – 7.14 (m, 1H), 7.04 – 6.97 (m, 1H), 6.90 – 6.84 (m, 1H), 4.59 (tt, J = 7.3, 3.5 Hz, 1H), 3.80 – 3.69 (m, 1H), 3.66 – 3.54 (m, 2H), 3.54 – 3.44 (m, 1H), 3.33 – 3.22 (m, 2H), 2.83 – 2.61 (m, 2H), 2.02 (s, 3H), 1.96 – 1.84 (m, 2H), 1.66 – 1.52 (m, 2H), 1.42 (s, 9H). ^{13}C NMR (101 MHz, DMSO-d_6) δ 170.7, 155.4, 153.9, 151.7, 142.0, 126.6, 125.1, 119.3, 112.1, 78.7, 71.9, 44.7, 31.1, 30.4, 28.1, 10.8. HRMS (ESI/[M+H]$^+$) Calcd for [$C_{21}H_{29}N_3O_5$+H]$^+$: 404.2180, found: 404.2182. HPLC purity: 96.3%.

3'-(2,4-dioxotetrahydropyrimidin-1(2H)-yl)-2'-methyl-[1,1'-biphenyl]-4-carbaldehyde (6I)—^{1}H NMR (400 MHz, DMSO-d_6) δ

10.38 (s, 1H), 10.08 (s, 1H), 8.04 – 7.97 (m, 2H), 7.62 – 7.55 (m, 2H), 7.41 – 7.35 (m, 2H), 7.29 – 7.20 (m, 1H), 3.89 – 3.77 (m, 1H), 3.62 – 3.52 (m, 1H), 2.87 – 2.75 (m, 1H), 2.75 – 2.65 (m, 1H), 2.09 (s, 3H). ^{13}C NMR (101 MHz, DMSO-d_6) δ 192.8, 170.7, 151.9, 147.0, 141.7, 141.5, 134.9, 133.1, 130.0, 129.5, 128.6, 127.2, 126.7, 44.7, 31.1, 15.3. HRMS (ESI/[M+H]$^+$) Calcd for [$C_{18}H_{16}N_2O_3$+H]$^+$: 309.1234, found: 309.1239. HPLC purity: 95.5%.

4-((3-(2,4-dioxotetrahydropyrimidin-1(2H)-yl)-2-methylphenoxy)methyl)benzaldehyde (6J)—^{1}H NMR (400 MHz, DMSO-d_6) δ 10.34 (s, 1H), 10.02 (s, 1H), 7.99 – 7.92 (m, 2H), 7.73 – 7.67 (m, 2H), 7.25 – 7.16 (m, 1H), 7.04 – 6.97 (m, 1H), 6.94 – 6.88 (m, 1H), 5.26 (s, 2H), 3.81 – 3.70 (m, 1H), 3.55 – 3.45 (m, 1H), 2.85 – 2.73 (m, 1H), 2.73 – 2.62 (m, 1H), 2.09 (s, 3H). ^{13}C NMR (101 MHz, DMSO-d_6) δ 192.8, 170.7, 156.5, 151.8, 144.2, 141.8, 135.6, 129.8, 127.6, 126.7, 124.3, 119.6, 110.8, 69.0, 44.7, 31.1, 10.8. HRMS (ESI/[M+H]$^+$) Calcd for [$C_{19}H_{18}N_2O_4$+H]$^+$: 339.1339, found: 339.1336. HPLC purity: 97.8%.

tert-butyl 2-(3-(2,4-dioxotetrahydropyrimidin-1(2H)-yl)-2-methylphenoxy)acetate (6K)—^{1}H NMR (400 MHz, DMSO-d_6) δ 10.33 (s, 1H), 7.21 – 7.13 (m, 1H), 6.93 – 6.87 (m, 1H), 6.83 – 6.76 (m, 1H), 4.70 (s, 2H), 3.80 – 3.69 (m, 1H), 3.54 – 3.43 (m, 1H), 2.84 – 2.72 (m, 1H), 2.72 – 2.61 (m, 1H), 2.05 (s, 3H). ^{13}C NMR (101 MHz, DMSO-d_6) δ 170.7, 167.8, 156.3, 151.7, 141.8, 126.5, 124.4, 119.8, 110.5, 81.4, 65.6, 44.7, 31.1, 27.7, 10.7. HRMS (ESI/[M+H]$^+$) Calcd for [$C_{17}H_{22}N_2O_5$+H]$^+$: 335.1601, found: 335.1604. HPLC purity: 96.4%.

tert-butyl 3-(3-(2,4-dioxotetrahydropyrimidin-1(2H)-yl)-2-methylphenyl)propanoate (6L)—^{1}H NMR (400 MHz, Acetone-d_6) δ 7.22 – 7.11 (m, 3H), 3.92 – 3.81 (m, 1H), 3.70 – 3.59 (m, 1H), 2.98 – 2.91 (m, 2H), 2.90 – 2.73 (m, 2H), 2.57 – 2.46 (m, 2H), 2.22 (s, 3H), 1.42 (s, 9H). ^{13}C NMR (101 MHz, Acetone-d_6) δ = 172.4, 170.9, 152.6, 142.4, 141.4, 135.0, 128.9, 127.2, 126.2, 80.4, 46.1, 36.2, 32.1, 29.5, 28.2, 13.8. HRMS (ESI/[M+H]$^+$) Calcd for [$C_{18}H_{24}N_2O_4$+H]$^+$: 333.1809, found: 333.1813. HPLC purity: 97.9%.

tert-butyl (E)-3-(3-(2,4-dioxotetrahydropyrimidin-1(2H)-yl)-2-methylphenyl)acrylate (6M)—^{1}H NMR (400 MHz, DMSO-d_6) δ 10.37 (s, 1H), 7.83 (d, J = 15.8 Hz, 1H), 7.71 – 7.65 (m, 1H), 7.38 – 7.33 (m, 1H), 7.33 – 7.24 (m, 1H), 6.42 (d, J = 15.8 Hz, 1H), 3.83 – 3.71 (m, 1H), 3.55 – 3.44 (m, 1H), 2.87 – 2.76 (m, 1H), 2.72 – 2.63 (m, 1H), 2.22 (s, 3H), 1.49 (s, 9H). ^{13}C NMR (101 MHz, DMSO-d_6) δ 170.7, 165.4, 152.0, 141.6, 140.9, 135.1, 134.3, 129.0, 126.8, 125.9, 121.8, 80.2, 44.6, 31.0, 27.8, 13.7. HRMS (ESI/[M+H]$^+$) Calcd for [$C_{18}H_{22}N_2O_4$+H]$^+$: 331.1652, found: 331.1665. HPLC purity: 99.6%.

1-(5-iodo-2-methylphenyl)dihydropyrimidine-2,4(1H,3H)-dione (7)—^{1}H NMR (400 MHz, DMSO-d_6) δ 10.42 (s, 1H), 7.67 (d, J = 1.9 Hz, 1H), 7.58 (dd, J = 8.0, 1.9 Hz, 1H), 7.09 (d, J = 8.1 Hz, 1H), 3.82 – 3.71 (m, 1H), 3.55 – 3.44 (m, 1H), 2.84 – 2.60 (m, 2H), 2.13 (s, 3H).^{13}C NMR (101 MHz, DMSO-d_6) δ 170.8, 151.7, 142.4, 136.1, 135.8, 135.7, 132.6, 90.7, 44.4, 31.1, 17.1.

1-(5-hydroxy-2-methylphenyl)dihydropyrimidine-2,4(1H,3H)-dione (7A)—^{1}H NMR (400 MHz, DMSO-d_6) δ 10.28 (s, 1H), 9.35 (s, 1H), 7.07 – 7.01 (m, 1H), 6.68 – 6.60 (m, 2H), 3.77 – 3.66 (m, 1H), 3.52 – 3.41 (m, 1H), 2.87 – 2.55 (m, 2H), 2.05 (s, 3H). ^{13}C NMR (101 MHz, DMSO-d_6) δ 170.8, 156.0, 151.6, 141.4, 131.0, 125.2, 114.5, 113.9, 44.5, 31.1, 16.6. HRMS (ESI/[M+H]$^+$) Calcd for [$C_{11}H_{12}N_2O_3$+H]$^+$: 221.0921, found: 221.0916. HPLC purity: 99.2%.

tert-butyl (3-(3-(2,4-dioxotetrahydropyrimidin-1(2H)-yl)-4-methylphenyl)prop-2-yn-1-yl)carbamate (7F)—^{1}H NMR (400 MHz, DMSO-d_6) δ 10.30 (s, 1H), 7.51 – 7.10 (m, 4H), 3.97 (d, J = 5.6 Hz, 2H), 3.82 – 3.71 (m, 1H), 3.54 – 3.43 (m, 1H), 2.80 – 2.60 (m, 2H), 2.18 (s, 3H), 1.39 (s, 9H). ^{13}C NMR (101 MHz, DMSO-d_6) δ 171.1, 155.3, 152.1, 141.3, 136.5, 130.9, 130.2, 130.1, 120.7, 87.6, 80.7, 78.3, 44.5, 31.2, 30.1, 28.2, 17.4. HRMS (ESI/[M+Na]$^+$) Calcd for [$C_{19}H_{23}N_3O_4$+Na]$^+$: 380.1581, found: 380.1598. HPLC purity: 99.1%.

tert-butyl (3-(3-(2,4-dioxotetrahydropyrimidin-1(2H)-yl)-4-methylphenyl)propyl)carbamate (7G)—^{1}H NMR (400 MHz, DMSO-d_6) δ 7.17 (d, J = 7.9 Hz, 1H), 7.05 (dd, J = 7.8, 1.8 Hz, 1H), 6.98 (d, J = 1.8 Hz, 1H), 5.97 (s, 1H), 4.68 (s, 1H), 3.82 – 3.71 (m, 1H), 3.63 – 3.53 (m, 1H), 3.17 – 3.07 (m, 2H), 2.77 (t, J = 6.8 Hz, 2H), 2.59 (t, J = 7.7 Hz, 2H), 2.20 (s, 3H), 1.77 (p, J = 7.3 Hz, 2H), 1.43 (s, 9H). ^{13}C NMR (101 MHz, DMSO-d_6) δ 171.3, 156.1, 152.9, 140.9, 140.2, 133.0, 131.3, 128.3, 126.9, 79.3, 77.4, 45.4, 40.0, 32.4, 31.6, 28.6, 17.6. HRMS (ESI/[M+H]$^+$) Calcd for [$C_{19}H_{27}N_3O_4$+H]$^+$: 362.2074, found: 362.2065. HPLC purity: 96.1%.

tert-butyl 4-(3-(2,4-dioxotetrahydropyrimidin-1(2H)-yl)-4-methylphenoxy)piperidine-1-carboxylate (7H)—^{1}H NMR (400 MHz, DMSO-d_6) δ 10.32 (s, 1H), 7.16 (d, J = 8.4 Hz, 1H), 6.91 (d, J = 2.6 Hz, 1H), 6.86 (dd, J = 8.4, 2.6 Hz, 1H), 4.50 (tt, J = 7.8, 3.6 Hz, 1H), 3.81 – 3.70 (m, 1H), 3.70 – 3.60 (m, 2H), 3.54 – 3.43 (m, 1H), 3.22 – 3.12 (m, 2H), 2.81 – 2.63 (m, 2H), 2.09 (s, 3H), 1.93 – 1.84 (m, 2H), 1.58 – 1.45 (m, 2H), 1.40 (s, 9H). ^{13}C NMR (101 MHz, DMSO-d_6) δ 170.8, 155.5, 153.9, 151.6, 141.7, 131.1, 127.4, 114.9, 114.8, 78.7, 72.0, 44.5, 31.1, 30.3, 28.1, 16.6. HRMS (ESI/[M+H]$^+$) Calcd for [$C_{21}H_{29}N_3O_5$+H]$^+$: 404.2180, found: 404.2196. HPLC purity: 96.4%.

3'-(2,4-dioxotetrahydropyrimidin-1(2H)-yl)-4'-methyl-[1,1'-biphenyl]-4-carbaldehyde (7I)—^{1}H NMR (400 MHz, DMSO-d_6) δ 10.40 (s, 1H), 10.05 (s, 1H), 8.03 – 7.96 (m, 2H), 7.96 – 7.89 (m, 2H), 7.75 (d, J = 2.0 Hz, 1H), 7.67 (dd, J = 7.9, 2.1 Hz, 1H), 7.42 (d, J = 8.1 Hz, 1H), 3.93 – 3.82 (m, 1H), 3.67 – 3.54 (m, 1H), 2.87 – 2.67 (m, 2H), 2.24 (s, 3H). ^{13}C NMR (101 MHz, DMSO-d_6) δ 192.7, 170.8, 151.8, 144.9, 141.7, 137.4, 136.2, 135.1, 131.4, 130.2, 127.1, 126.0, 125.9, 44.6, 31.2, 17.3. HRMS (ESI/[M+H]$^+$) Calcd for [$C_{18}H_{16}N_2O_3$+H]$^+$: 309.1234, found: 309.1239. HPLC purity: 95.2%.

4-((3-(2,4-dioxotetrahydropyrimidin-1(2H)-yl)-4-methylphenoxy)methyl)benzaldehyde (7J)—^{1}H NMR (400 MHz, DMSO-d_6) δ 10.34 (s, 1H), 10.01 (s, 1H), 7.97 – 7.90 (m, 2H), 7.70 – 7.63 (m, 2H), 7.18 (d, J = 8.5 Hz, 1H), 7.01 (d, J = 2.7 Hz, 1H), 6.92 (dd, J = 8.4, 2.7 Hz, 1H), 5.20 (s, 2H), 3.82 – 3.71 (m, 1H), 3.54 – 3.44 (m, 1H), 2.82 – 2.62

(m, 2H), 2.10 (s, 3H). ^{13}C NMR (101 MHz, DMSO-d_6) δ 192.8, 170.8, 156.8, 151.6, 143.9, 141.6, 135.6, 131.1, 129.7, 127.8, 127.8, 113.8, 113.8, 68.7, 44.5, 31.1, 16.6. HRMS (ESI/[M+H]$^+$) Calcd for [$C_{19}H_{18}N_2O_4$+H]$^+$: 339.1339, found: 339.1334. HPLC purity: 98.4%.

tert-butyl 2-(3-(2,4-dioxotetrahydropyrimidin-1(2H)-yl)-4-methylphenoxy)acetate (7K)—^{1}H NMR (400 MHz, DMSO-d_6) δ 10.32 (s, 1H), 7.17 (d, J = 8.4 Hz, 1H), 6.87 (d, J = 2.7 Hz, 1H), 6.78 (dd, J = 8.4, 2.7 Hz, 1H), 4.62 (s, 2H), 3.81 – 3.70 (m, 1H), 3.53 – 3.43 (m, 1H), 2.86 – 2.57 (m, 2H), 2.10 (s, 3H), 1.43 (s, 9H). ^{13}C NMR (101 MHz, DMSO-d_6) δ 170.7, 167.8, 156.3, 151.6, 141.5, 131.0, 127.9, 113.5, 113.4, 81.4, 65.2, 44.5, 31.1, 27.7, 16.6. HRMS (ESI/[M+H]$^+$) Calcd for [$C_{17}H_{22}N_2O_5$+H]$^+$: 335.1601, found: 335.1592. HPLC purity: 97.5%.

tert-butyl 3-(3-(2,4-dioxotetrahydropyrimidin-1(2H)-yl)-4-methylphenyl)propanoate (7L)—^{1}H NMR (400 MHz, $CDCl_3$) δ 7.43 (s, 1H), 7.21 (d, J = 7.8 Hz, 1H), 7.11 (dd, J = 7.8, 1.8 Hz, 1H), 7.02 (d, J = 1.8 Hz, 1H), 3.86 – 3.74 (m, 1H), 3.68 – 3.57 (m, 1H), 2.93 – 2.79 (m, 4H), 2.53 (t, J = 7.1 Hz, 2H), 2.23 (s, 3H), 1.42 (s, 9H). ^{13}C NMR (101 MHz, DMSO-d_6) δ 171.5, 170.8, 151.6, 140.7, 139.3, 133.0, 130.4, 127.3, 126.8, 79.7, 44.6, 36.1, 31.2, 29.8, 27.7, 17.1. HRMS (ESI/[M+H]$^+$) Calcd for [$C_{18}H_{24}N_2O_4$+H]$^+$: 333.1809, found: 333.1802. HPLC purity: 97.9%.

tert-butyl (E)-3-(3-(2,4-dioxotetrahydropyrimidin-1(2H)-yl)-4-methylphenyl)acrylate (7M)—^{1}H NMR (400 MHz, DMSO-d_6) δ 10.38 (s, 1H), 7.69 (d, J = 1.8 Hz, 1H), 7.57 – 7.47 (m, 2H), 7.31 (d, J = 8.0 Hz, 1H), 6.52 (d, J = 15.9 Hz, 1H), 3.86 – 3.75 (m, 1H), 3.58 – 3.48 (m, 1H), 2.84 – 2.66 (m, 2H), 2.20 (s, 3H), 1.48 (s, 9H). ^{13}C NMR (101 MHz, DMSO-d_6) δ 170.8, 165.5, 151.7, 142.7, 141.5, 138.1, 133.1, 131.1, 127.5, 126.7, 119.7, 79.9, 44.6, 31.1, 27.8, 17.5. HRMS (ESI/[M+H]$^+$) Calcd for [$C_{18}H_{22}N_2O_4$+H]$^+$: 331.1652, found: 331.1647. HPLC purity: 98.5%.

1-(4-hydroxy-2-methylphenyl)dihydropyrimidine-2,4(1H,3H)-dione (8A)—^{1}H NMR (400 MHz, DMSO-d_6) δ ^{1}H NMR (400 MHz, DMSO) δ 10.23 (s, 1H), 9.40 (s, 1H), 7.01 (d, J = 8.5 Hz, 1H), 6.64 (d, J = 2.8 Hz, 1H), 6.60 (dd, J = 8.4, 2.8 Hz, 1H), 3.71 – 3.60 (m, 1H), 3.50 – 3.39 (m, 1H), 2.79 – 2.59 (m, 2H), 2.08 (s, 3H). ^{13}C NMR (101 MHz, DMSO-d_6) δ 170.8, 156.4, 152.0, 136.5, 132.3, 128.2, 116.8, 113.3, 44.9, 31.2, 17.5. HRMS (ESI/[M+H]$^+$) Calcd for [$C_{11}H_{12}N_2O_3$+H]$^+$: 221.0921, found: 221.0916. HPLC purity: 97.9%.

tert-butyl 4-(4-(2,4-dioxotetrahydropyrimidin-1(2H)-yl)-3-methylphenoxy)piperidine-1-carboxylate (8H)—^{1}H NMR (400 MHz, DMSO-d_6) δ 10.28 (s, 1H), 7.14 (d, J = 8.6 Hz, 1H), 6.88 (d, J = 2.9 Hz, 1H), 6.82 (dd, J = 8.6, 2.9 Hz, 1H), 4.54 (tt, J = 7.8, 3.6 Hz, 1H), 3.73 – 3.60 (m, 3H), 3.52 – 3.42 (m, 1H), 3.23 – 3.14 (m, 2H), 2.80 – 2.60 (m, 2H), 2.14 (s, 3H), 1.94 – 1.84 (m, 2H), 1.58 – 1.45 (m, 2H), 1.41 (s, 9H). ^{13}C NMR (101 MHz, DMSO-d_6) δ 170.8, 155.8, 153.9, 151.9, 136.9, 133.9, 128.3, 117.5, 113.7, 78.7, 71.9, 44.8, 31.1, 30.4, 28.1, 17.6. HRMS (ESI/[M+H]$^+$) Calcd for [$C_{21}H_{29}N_3O_5$+H]$^+$: 404.2180, found: 404.2169. HPLC purity: 96.3%.

4-((4-(2,4-dioxotetrahydropyrimidin-1(2H)-yl)-3-methylphenoxy)methyl)benzaldehyde (8J)—^{1}H NMR (400 MHz, DMSO-d_6) δ 10.29 (s, 1H), 10.01 (s, 1H), 7.97 – 7.91 (m, 2H), 7.70 – 7.64 (m, 2H), 7.17 (d, J = 8.6 Hz, 1H), 6.96 (d, J = 2.9 Hz, 1H), 6.88 (dd, J = 8.6, 3.0 Hz, 1H), 5.23 (s, 2H), 3.75 – 3.64 (m, 1H), 3.52 – 3.41 (m, 1H), 2.81 – 2.60 (m, 2H), 2.15 (s, 3H). ^{13}C NMR (101 MHz, DMSO-d_6) δ 192.8, 170.8, 156.9, 151.9, 144.1, 136.9, 135.6, 134.2, 129.7, 128.4, 127.7, 116.5, 112.8, 68.6, 44.8, 31.1, 17.6. HRMS (ESI/[M+H]$^+$) Calcd for [$C_{19}H_{18}N_2O_4$+H]$^+$: 339.1339, found: 339.1335. HPLC purity: 98.5%.

tert-butyl 2-(4-(2,4-dioxotetrahydropyrimidin-1(2H)-yl)-3-methylphenoxy)acetate (8K)—^{1}H NMR (400 MHz, DMSO-d_6) δ 10.28 (s, 1H), 7.16 (d, J = 8.6 Hz, 1H), 6.81 (d, J = 3.0 Hz, 1H), 6.75 (dd, J = 8.6, 3.0 Hz, 1H), 4.64 (s, 2H), 3.75 – 3.64 (m, 1H), 3.52 – 3.42 (m, 1H), 2.81 – 2.60 (m, 2H), 2.14 (s, 3H), 1.44 (s, 9H). ^{13}C NMR (101 MHz, DMSO-d_6) δ170.8, 167.8, 156.5, 151.9, 136.8, 134.3, 128.2, 116.2, 112.4, 81.4, 65.0, 44.8, 31.1, 27.7, 17.6. HRMS (ESI/[M+H]$^+$) Calcd for [$C_{17}H_{22}N_2O_5$+H]$^+$: 335.1601, found: 335.1593. HPLC purity: 95.8%.

1-(2-methyl-3-(2-oxo-2-(piperidin-1-yl)ethoxy)phenyl)dihydropyrimidine-2,4(1H,3H)-dione (9)—^{1}H NMR (400 MHz, DMSO-d_6) δ 10.32 (s, 1H), 7.20 – 7.12 (m, 1H), 6.91 – 6.80 (m, 2H), 3.80 – 3.69 (m, 1H), 3.53 – 3.35 (m, 5H), 2.84 – 2.61 (m, 2H), 2.04 (s, 3H), 1.64–1.39 (m, 6H). ^{13}C NMR (101 MHz, DMSO-d_6) 170.7, 165.4, 156.6, 151.7, 141.7, 126.5, 124.1, 119.4, 110.6, 66.7, 45.2, 44.7, 42.2, 31.1, 26.0, 25.3, 24.0, 10.8. HRMS (ESI/[M+H]$^+$) Calcd for [$C_{18}H_{23}N_3O_4$+H]$^+$: 346.1761, found: 346.1760. HPLC purity: 98.9%.

2-(3-(2,4-dioxotetrahydropyrimidin-1(2H)-yl)-2-methylphenoxy)-N-ethylacetamide (10)—^{1}H NMR (400 MHz, DMSO-d_6) δ 10.33 (s, 1H), 8.08 – 7.91 (m, 1H), 7.23 – 7.14 (m, 1H), 6.95 – 6.88 (m, 1H), 6.86 – 6.79 (m, 1H), 4.48 (s, 2H), 3.80 – 3.69 (m, 1H), 3.54 – 3.43 (m, 1H), 3.23 – 3.12 (m, 2H), 2.84 – 2.62 (m, 2H), 2.09 (s, 3H), 1.05 (t, J = 7.2 Hz, 3H). ^{13}C NMR (101 MHz, DMSO-d_6) δ 170.7, 167.3, 156.5, 151.8, 141.8, 126.6, 124.6, 119.9, 110.8, 67.7, 44.7, 33.3, 31.1, 14.8, 10.9. HRMS (ESI/[M+H]$^+$) Calcd for [$C_{15}H_{19}N_3O_4$+H]$^+$: 306.1448, found: 306.1444. HPLC purity: 99.1%.

N-(4-(3-(2,4-dioxotetrahydropyrimidin-1(2H)-yl)-2-methylphenyl)but-3-yn-1-yl)acetamide (11)—^{1}H NMR (400 MHz, DMSO-d_6) δ 10.36 (s, 1H), 8.11 – 8.04 (m, 1H), 7.38 – 7.32 (m, 1H), 7.30 – 7.18 (m, 2H), 3.82 – 3.71 (m, 1H), 3.55 – 3.45 (m, 1H), 3.25 (t, J = 6.9 Hz, 2H), 2.85 – 2.72 (m, 1H), 2.75 – 2.62 (m, 1H), 2.59 (t, J = 6.9 Hz, 2H), 2.24 (s, 3H), 1.82 (s, 3H). ^{13}C NMR (101 MHz, DMSO-d_6) δ 170.7, 169.3, 151.8, 141.2, 137.5, 130.8, 127.3, 126.6, 124.2, 92.7, 79.7, 44.5, 37.9, 31.1, 22.6, 19.9, 15.7. HRMS (ESI/[M+H]$^+$) Calcd for [$C_{17}H_{19}N_3O_3$+H]$^+$: 314.1499, found: 314.1491. HPLC purity: 95.4%.

(S)-2-(4-(4-chlorophenyl)-2,3,9-trimethyl-6H-thieno[3,2-f][1,2,4]triazolo[4,3-a][1,4]diazepin-6-yl)-N-(3-(3-(2,4-dioxotetrahydropyrimidin-1(2H)-yl)-2-methylphenyl)prop-2-yn-1-yl)acetamide (12A)—^{1}H NMR (400 MHz, $CDCl_3$) δ 8.07 (d, J = 5.3 Hz, 1H), 7.42 – 7.36 (m, 3H), 7.35 – 7.30 (m, 1H), 7.25 – 7.13 (m, 4H), 4.68 – 4.60 (m, 1H), 4.50 – 4.38 (m, 1H),

4.29 – 4.17 (m, 1H), 3.81 – 3.68 (m, 1H), 3.63 – 3.40 (m, 3H), 2.84 – 2.75 (m, 2H), 2.65 (d, *J* = 1.5 Hz, 3H), 2.39 (s, 3H), 2.28 (d, *J* = 3.7 Hz, 3H), 1.68 – 1.62 (m, 3H). ^{13}C NMR (101 MHz, $CDCl_3$) δ ^{13}C NMR (101 MHz, $CDCl_3$) δ 170.4, 169.7, 164.2, 155.6, 151.6, 150.1, 140.1, 138.2, 136.8, 136.7, 132.4, 132.3, 131.0, 131.0, 130.5, 130.0, 128.8, 127.4, 126.9, 124.9, 90.1, 81.4, 54.5, 45.3, 39.1, 31.5, 30.2, 16.2, 14.5, 13.2, 11.9. HRMS (ESI/[M+H]$^+$) Calcd for $[C_{33}H_{30}ClN_7O_3S+H]^+$: 640.1892, found: 640.1883. HPLC purity: 96.0%.

(S)-2-(4-(4-chlorophenyl)-2,3,9-trimethyl-6H-thieno[3,2-f][1,2,4]triazolo[4,3-a][1,4]diazepin-6-yl)-N-(4-(3-(2,4-dioxotetrahydropyrimidin-1(2H)-yl)-2-methylphenyl)but-3-yn-1-yl)acetamide (12B)—^{1}H NMR (400 MHz, MeOD-*d*$_4$) δ 7.50 – 7.41 (m, 2H), 7.39 – 7.27 (m, 3H), 7.26 – 7.13 (m, 2H), 4.69 (dd, *J* = 8.8, 5.2 Hz, 1H), 3.86 – 3.69 (m, 1H), 3.65 – 3.42 (m, 4H), 3.38 – 3.32 (m, 2H), 2.91 – 2.73 (m, 3H), 2.71 (s, 3H), 2.43 (s, 3H), 2.31 (s, 3H), 1.73 – 1.63 (m, 3H). ^{13}C NMR (101 MHz, MeOD-*d*$_4$) δ 172.8, 172.8, 166.5, 156.9, 154.1, 152.4, 141.9, 139.2, 138.2, 137.8, 133.7, 133.3, 132.9, 132.2, 132.0, 131.4, 129.8, 128.2, 127.8, 126.6, 93.2, 81.0, 55.0, 46.3, 39.9, 38.5, 32.1, 21.0, 16.3, 14.4, 13.0, 11.6. HRMS (ESI/[M+H]$^+$) Calcd for $[C_{34}H_{32}ClN_7O_3S+H]^+$: 654.2049, found: 654.2031. HPLC purity: 95.6%.

(S)-2-(4-(4-chlorophenyl)-2,3,9-trimethyl-6H-thieno[3,2-f][1,2,4]triazolo[4,3-a][1,4]diazepin-6-yl)-N-(5-(3-(2,4-dioxotetrahydropyrimidin-1(2H)-yl)-2-methylphenyl)pent-4-yn-1-yl)acetamide (12C)—^{1}H NMR (101 MHz, MeOD-*d*$_4$) δ 7.51 – 7.44 (m, 2H), 7.44 – 7.29 (m, 3H), 7.25 – 7.15 (m, 2H), 4.69 (dd, *J* = 9.0, 5.3 Hz, 1H), 3.87 – 3.76 (m, 1H), 3.67 – 3.57 (m, 1H), 3.54 – 3.37 (m, 3H), 3.36 – 3.26 (m, 1H), 2.93 – 2.70 (m, 2H), 2.73 (s, 3H), 2.59 (t, *J* = 7.1 Hz, 2H), 2.45 (s, 3H), 2.32 (d, *J* = 11.6 Hz, 3H), 1.90 (p, *J* = 6.9 Hz, 2H), 1.73 – 1.67 (m, 3H). ^{13}C NMR (101 MHz, MeOD-*d*$_4$) δ 172.9, 172.7, 166.6, 156.9, 154.2, 152.5, 141.9, 139.0, 138.3, 137.7, 133.8, 133.4, 132.8, 132.2, 132.0, 131.5, 129.9, 128.0, 127.8, 126.8, 95.1, 80.5, 55.1, 46.3, 39.6, 38.5, 32.1, 29.7, 17.7, 16.3, 14.4, 12.9, 11.5. HRMS (ESI/[M+H]$^+$) Calcd for $[C_{35}H_{34}ClN_7O_3S+H]^+$: 668.2205, found: 668.2195. HPLC purity: 96.7%.

(S)-2-(4-(4-chlorophenyl)-2,3,9-trimethyl-6H-thieno[3,2-f][1,2,4]triazolo[4,3-a][1,4]diazepin-6-yl)-N-(1-(2-(3-(2,4-dioxotetrahydropyrimidin-1(2H)-yl)-2-methylphenoxy)acetyl)piperidin-4-yl)acetamide (13)—^{1}H NMR (400 MHz, Acetone-*d*$_6$) δ 7.53 – 7.38 (m, 4H), 7.22 – 7.10 (m, 1H), 7.04 – 6.85 (m, 2H), 4.98 – 4.76 (m, 2H), 4.68 – 4.57 (m, 1H), 4.41 – 4.20 (m, 1H), 4.12 – 3.79 (m, 3H), 3.77 – 3.59 (m, 1H), 3.43 – 3.16 (m, 3H), 2.89 – 2.72 (m, 3H), 2.61 (s, 3H), 2.45 (s, 3H), 2.15 (s, 3H), 2.01 – 1.78 (m, 2H), 1.70 (s, 3H), 1.62 – 1.34 (m, 2H). ^{13}C NMR (101 MHz, Acetone-*d*$_6$) δ 171.0, 170.1, 166.6, 164.2, 157.9, 156.5, 152.5, 150.6, 142.9, 138.3, 136.7, 133.6, 131.7, 131.2, 131.1, 131.0, 129.3, 127.5, 125.8, 120.5, 111.6, 68.4, 55.2, 47.1, 46.0, 44.5, 41.4, 39.1, 33.1, 32.6, 32.1, 14.5, 13.0, 11.8, 11.3. HRMS (ESI/[M+H]$^+$) Calcd for $[C_{37}H_{39}ClN_8O_5S+H]^+$: 743.2525, found: 743.2504. HPLC purity: 96.0%.

(S)-2-(4-(4-chlorophenyl)-2,3,9-trimethyl-6H-thieno[3,2-f][1,2,4]triazolo[4,3-a][1,4]diazepin-6-yl)-N-(1-(2-(2-methyl-3-(3-methyl-2,4-dioxotetrahydropyrimidin-1(2H)-yl)phenoxy)acetyl)piperidin-4-yl)acetamide

(13NT)—^{1}H NMR (400 MHz, Acetone-d_6) δ 7.52 – 7.45 (m, 2H), 7.44 – 7.38 (m, 2H), 7.21 – 7.13 (m, 1H), 6.98 – 6.88 (m, 2H), 5.02 – 4.73 (m, 2H), 4.69–4.57 (m, 1H), 4.31 (d, J = 11.3 Hz, 1H), 4.10 – 3.92 (m, 2H), 3.90 – 3.76 (m, 1H), 3.67 – 3.56 (m, 1H), 3.45 – 3.18 (m, 3H), 3.10 (s, 3H), 2.98 – 2.75 (m, 3H), 2.61 (s, 3H), 2.44 (s, 3H), 2.15 (s, 3H), 2.02 – 1.78 (m, 2H), 1.70 (s, 3H), 1.64 – 1.38 (m, 2H). ^{1}H NMR (400 MHz, Acetone-d_6) δ 170.3, 170.1, 166.6, 164.2, 157.9, 156.5, 153.6, 150.6, 143.6, 138.2, 136.7, 133.6, 131.7, 131.2, 131.1, 131.0, 129.3, 127.5, 125.7, 120.5, 111.6, 68.5, 55.2, 47.0, 44.8, 44.6, 41.5, 39.2, 32.9, 32.5, 32.2, 27.6, 14.5, 13.0, 11.8, 11.3. HRMS (ESI/[M+H]$^{+}$) Calcd for $[C_{38}H_{41}ClN_8O_5S+H]^{+}$: 757.2682, found: 757.2662. HPLC purity: 97.2%.

(S)-N-(2-(1-(2-(4-(4-chlorophenyl)-2,3,9-trimethyl-6H-thieno[3,2-f][1,2,4]triazolo[4,3-a][1,4]diazepin-6-yl)acetyl)piperidin-4-yl)ethyl)-2-(3-(2,4-dioxotetrahydropyrimidin-1(2H)-yl)-2-methylphenoxy)acetamide (14)—^{1}H NMR (400 MHz, Acetone-d_6) δ 9.19 (t, J = 4.3 Hz, 1H), 7.53 – 7.45 (m, 3H), 7.45 – 7.38 (m, 2H), 7.27 – 7.18 (m, 1H), 7.01 – 6.95 (m, 1H), 6.92 – 6.86 (m, 1H), 4.71 (t, J = 6.6 Hz, 1H), 4.56 – 4.45 (m, 3H), 4.23 – 4.15 (m, 1H), 3.95 – 3.83 (m, 1H), 3.70 – 3.55 (m, 2H), 3.48 – 3.37 (m, 1H), 3.40 – 3.31 (m, 2H), 3.16 – 3.03 (m, 1H), 2.89 – 2.69 (m, 2H), 2.61 (s, 3H), 2.58 – 2.47 (m, 1H), 2.44 (s, 3H), 2.16 (s, 3H), 1.92 – 1.41 (m, 8H), 1.23 (s, 1H), 1.13 – 0.93 (m, 1H). ^{13}C NMR (101 MHz, Acetone-d_6) δ 170.9, 168.9, 168.5, 163.9, 157.5, 156.7, 152.5, 150.4, 143.1, 138.4, 136.6, 133.6, 131.6, 131.2, 131.1, 131.0, 129.3, 127.7, 126.0, 121.0, 111.6, 68.9, 55.6, 46.5, 46.0, 42.6, 36.9, 36.9, 36.0, 34.5, 33.5, 32.7, 32.1, 14.5, 13.0, 11.7, 11.3. HRMS (ESI/[M+H]$^{+}$) Calcd for $[C_{39}H_{43}ClN_8O_5S+H]^{+}$: 771.2838, found: 771.2822. HPLC purity: 95.4%.

Supplementary Material

Refer to Web version on PubMed Central for supplementary material.

ACKNOWLEDGMENT

W.T. thanks the financial support from the University of Wisconsin– Madison Office of the Vice Chancellor for Research and Graduate Education with funding from the Wisconsin Alumni Research Foundation (WARF) through a UW2020 award before June 30, 2022 and National Institute of General Medical Sciences of the National Institutes of Health under award number R35GM148266. I.T. thanks NIH T32 GM141013 for the pre-doctoral fellowship. This study made use of the Medicinal Chemistry Center at UW-Madison instrumentation funded by the UW Lachman Institute for Pharmaceutical Development at the School of Pharmacy and WARF, and UW Carbone Cancer Center Flow Cytometry Core. We thank Eric Fischer's lab from Dana-Farber Cancer Institute, Harvard University, for DNA plasmid: BRD4(BD1) subcloned into mammalian pcDNA5/FRT Vector (Ampicillin and Hygromycin B resistant) modified to contain MCS-eGFP-P2A-mCherry.

Funding Sources

NIH R35GM148266

NIH T32 GM141013

ABBREVIATIONS

CRBN	cereblon
TLC	thin layer chromatography

PROTAC	proteolysis targeting chimeras
PDHU	phenyl dihydrouracil
MD	molecular dynamics
BRD4	Bromodomain-containing protein 4
BD1	bromodomain 1
GFP	green fluorescent protein
POI	protein of interest
SAR	structure-activity relationship
DDB1	DNA damage-binding protein 1
DIPEA	*N,N*-diisopropylethylamine
HATU	O-(7-Azabenzotriazol-1-yl)-*N,N,N',N'*-tetramethyluronium hexafluorophosphate

REFERENCES

(1). Schapira M; Calabrese MF; Bullock AN; Crews CM Targeted Protein Degradation: Expanding the Toolbox. Nat. Rev. Drug Discov 2019, 18 (12), 949–963. 10.1038/s41573-019-0047-y. [PubMed: 31666732]

(2). Luh LM; Scheib U; Juenemann K; Wortmann L; Brands M; Cromm PM Prey for the Proteasome: Targeted Protein Degradation—A Medicinal Chemist's Perspective. Angew. Chem. Int. Ed 2020, 59 (36), 15448–15466. 10.1002/anie.202004310.

(3). Dale B; Cheng M; Park K-S; Kaniskan HÜ; Xiong Y; Jin J Advancing Targeted Protein Degradation for Cancer Therapy. Nat. Rev. Cancer 2021, 21 (10), 638–654. 10.1038/s41568-021-00365-x. [PubMed: 34131295]

(4). Mullard A Targeted Protein Degraders Crowd into the Clinic. Nat. Rev. Drug Discov 2021, 20 (4), 247–250. 10.1038/d41573-021-00052-4. [PubMed: 33737725]

(5). Békés M; Langley DR; Crews CM PROTAC Targeted Protein Degraders: The Past Is Prologue. Nat. Rev. Drug Discov 2022, 21 (3), 181–200. 10.1038/s41573-021-00371-6. [PubMed: 35042991]

(6). Lai AC; Crews CM Induced Protein Degradation: An Emerging Drug Discovery Paradigm. Nat. Rev. Drug Discov 2017, 16 (2), 101–114. 10.1038/nrd.2016.211. [PubMed: 27885283]

(7). Sakamoto KM; Kim KB; Kumagai A; Mercurio F; Crews CM; Deshaies RJ Protacs: Chimeric Molecules That Target Proteins to the Skp1–Cullin–F Box Complex for Ubiquitination and Degradation. Proc. Natl. Acad. Sci 2001, 98 (15), 8554–8559. 10.1073/pnas.141230798. [PubMed: 11438690]

(8). Lipinski CA Drug-like Properties and the Causes of Poor Solubility and Poor Permeability. J. Pharmacol. Toxicol. Methods 2000, 44 (1), 235–249. 10.1016/S1056-8719(00)00107-6. [PubMed: 11274893]

(9). Lipinski CA Lead- and Drug-like Compounds: The Rule-of-Five Revolution. Drug Discov. Today Technol 2004, 1 (4), 337–341. 10.1016/j.ddtec.2004.11.007. [PubMed: 24981612]

(10). Leeson PD; Springthorpe B The Influence of Drug-like Concepts on Decision-Making in Medicinal Chemistry. Nat. Rev. Drug Discov 2007, 6 (11), 881–890. 10.1038/nrd2445. [PubMed: 17971784]

(11). Doak BC; Over B; Giordanetto F; Kihlberg J Oral Druggable Space beyond the Rule of 5: Insights from Drugs and Clinical Candidates. Chem. Biol 2014, 21 (9), 1115–1142. 10.1016/j.chembiol.2014.08.013. [PubMed: 25237858]

(12). Wang C; Zhang Y; Wu Y; Xing D Developments of CRBN-Based PROTACs as Potential Therapeutic Agents. Eur. J. Med. Chem 2021, 225, 113749. 10.1016/j.ejmech.2021.113749. [PubMed: 34411892]

(13). Winter GE; Buckley DL; Paulk J; Roberts JM; Souza A; Dhe-Paganon S; Bradner JE Phthalimide Conjugation as a Strategy for in Vivo Target Protein Degradation. Science 2015, 348 (6241), 1376–1381. 10.1126/science.aab1433. [PubMed: 25999370]

(14). Lu J; Qian Y; Altieri M; Dong H; Wang J; Raina K; Hines J; Winkler JD; Crew AP; Coleman K; Crews CM Hijacking the E3 Ubiquitin Ligase Cereblon to Efficiently Target BRD4. Chem. Biol 2015, 22 (6), 755–763. 10.1016/j.chembiol.2015.05.009. [PubMed: 26051217]

(15). Eriksson T; Björkman S; Roth B; Fyge Å; Höuglund P Stereospecific Determination, Chiral Inversion in Vitro and Pharmacokinetics in Humans of the Enantiomers of Thalidomide. Chirality 1995, 7 (1), 44–52. 10.1002/chir.530070109. [PubMed: 7702998]

(16). Chamberlain PP; Lopez-Girona A; Miller K; Carmel G; Pagarigan B; Chie-Leon B; Rychak E; Corral LG; Ren YJ; Wang M; Riley M; Delker SL; Ito T; Ando H; Mori T; Hirano Y; Handa H; Hakoshima T; Daniel TO; Cathers BE Structure of the Human Cereblon–DDB1–Lenalidomide Complex Reveals Basis for Responsiveness to Thalidomide Analogs. Nat. Struct. Mol. Biol 2014, 21 (9), 803–809. 10.1038/nsmb.2874. [PubMed: 25108355]

(17). Mori T; Ito T; Liu S; Ando H; Sakamoto S; Yamaguchi Y; Tokunaga E; Shibata N; Handa H; Hakoshima T Structural Basis of Thalidomide Enantiomer Binding to Cereblon. Sci. Rep 2018, 8 (1), 1294. 10.1038/s41598-018-19202-7. [PubMed: 29358579]

(18). Fischer ES; Böhm K; Lydeard JR; Yang H; Stadler MB; Cavadini S; Nagel J; Serluca F; Acker V; Lingaraju GM; Tichkule RB; Schebesta M; Forrester WC; Schirle M; Hassiepen U; Ottl J; Hild M; Beckwith REJ; Harper JW; Jenkins JL; Thomä NH Structure of the DDB1–CRBN E3 Ubiquitin Ligase in Complex with Thalidomide. Nature 2014, 512 (7512), 49. 10.1038/nature13527. [PubMed: 25043012]

(19). FDA'S Policy Statement for the Development of New Stereoisomeric Drugs. Chirality 1992, 4 (5), 338–340. 10.1002/chir.530040513. [PubMed: 1354468]

(20). Kazantsev A; Krasavin M Ligands for Cereblon: 2017–2021 Patent Overview. Expert Opin. Ther. Pat 2022, 32 (2), 171–190. 10.1080/13543776.2022.1999415. [PubMed: 34704527]

(21). Jacques V; Czarnik AW; Judge TM; Van der Ploeg LHT; DeWitt SH Differentiation of Antiinflammatory and Antitumorigenic Properties of Stabilized Enantiomers of Thalidomide Analogs. Proc. Natl. Acad. Sci 2015, 112 (12), E1471–E1479. 10.1073/pnas.1417832112. [PubMed: 25775521]

(22). Hartmann MD; Boichenko I; Coles M; Zanini F; Lupas AN; Hernandez Alvarez B Thalidomide Mimics Uridine Binding to an Aromatic Cage in Cereblon. J. Struct. Biol 2014, 188 (3), 225–232. 10.1016/j.jsb.2014.10.010. [PubMed: 25448889]

(23). Boichenko I; Bär K; Deiss S; Heim C; Albrecht R; Lupas AN; Hernandez Alvarez B; Hartmann MD Chemical Ligand Space of Cereblon. ACS Omega 2018, 3 (9), 11163–11171. 10.1021/acsomega.8b00959. [PubMed: 31459225]

(24). Sosič I; Bricelj A; Steinebach C E3 Ligase Ligand Chemistries: From Building Blocks to Protein Degraders. Chem. Soc. Rev 2022. 10.1039/D2CS00148A.

(25). Yamamoto T; Tokunaga E; Nakamura S; Shibata N; Toru T Synthesis and Configurational Stability of (*S*)- and (*R*)-Deuteriothalidomides. Chem. Pharm. Bull. (Tokyo) 2010, 58 (1), 110–112. 10.1248/cpb.58.110. [PubMed: 20045977]

(26). Hansen JD; Correa M; Nagy MA; Alexander M; Plantevin V; Grant V; Whitefield B; Huang D; Kercher T; Harris R; Narla RK; Leisten J; Tang Y; Moghaddam M; Ebinger K; Piccotti J; Havens CG; Cathers B; Carmichael J; Daniel T; Vessey R; Hamann LG; Leftheris K; Mendy D; Baculi F; LeBrun LA; Khambatta G; Lopez-Girona A Discovery of CRBN E3 Ligase Modulator CC-92480 for the Treatment of Relapsed and Refractory Multiple Myeloma. J. Med. Chem 2020, 63 (13), 6648–6676. 10.1021/acs.jmedchem.9b01928. [PubMed: 32130004]

(27). Nishimura K; Hashimoto Y; Iwasaki S (S)-Form of α-Methyl-N(α)-Phthalimidoglutarimide, But not Its (R)-Form, Enhanced Phorbol Ester-Induced Tumor Necrosis Factor-α Production by Human Leukemia Cell HL-60 : Important of Optical Resolution of Thalidomidal Effects. Chem. Pharm. Bull. (Tokyo) 1994, 42 (5), 1157–1159. 10.1248/cpb.42.1157. [PubMed: 8069968]

(28). Min J; Mayasundari A; Keramatnia F; Jonchere B; Yang SW; Jarusiewicz J; Actis M; Das S; Young B; Slavish J; Yang L; Li Y; Fu X; Garrett SH; Yun M-K; Li Z; Nithianantham S; Chai S; Chen T; Shelat A; Lee RE; Nishiguchi G; White SW; Roussel MF; Potts PR; Fischer M; Rankovic Z Phenyl-Glutarimides: Alternative Cereblon Binders for the Design of PROTACs. Angew. Chem. Int. Ed 2021, 60 (51), 26663–26670. 10.1002/anie.202108848.

(29). Fromme JC; Verdine GL DNA Lesion Recognition by the Bacterial Repair Enzyme MutM*. J. Biol. Chem 2003, 278 (51), 51543–51548. 10.1074/jbc.M307768200. [PubMed: 14525999]

(30). Barreiro EJ; Kümmerle AE; Fraga CAM The Methylation Effect in Medicinal Chemistry. Chem. Rev 2011, 111 (9), 5215–5246. 10.1021/cr200060g. [PubMed: 21631125]

(31). Leung CS; Leung SSF; Tirado-Rives J; Jorgensen WL Methyl Effects on Protein–Ligand Binding. J. Med. Chem 2012, 55 (9), 4489–4500. 10.1021/jm3003697. [PubMed: 22500930]

(32). Liao J; Nie X; Unarta IC; Ericksen SS; Tang W In Silico Modeling and Scoring of PROTAC-Mediated Ternary Complex Poses. J. Med. Chem 2022, 65 (8), 6116–6132. 10.1021/acs.jmedchem.1c02155. [PubMed: 35412837]

(33). Schumacher H; Smith RL; Williams RT The Metabolism of Thalidomide: The Spontaneous Hydrolysis of Thalidomide in Solution. Br. J. Pharmacol. Chemother 1965, 25 (2), 324–337. 10.1111/j.1476-5381.1965.tb02053.x. [PubMed: 5866715]

(34). Franks ME; Macpherson GR; Figg WD Thalidomide. The Lancet 2004, 363 (9423), 1802–1811. 10.1016/S0140-6736(04)16308-3.

(35). Nowak RP; DeAngelo SL; Buckley D; He Z; Donovan KA; An J; Safaee N; Jedrychowski MP; Ponthier CM; Ishoey M; Zhang T; Mancias JD; Gray NS; Bradner JE; Fischer ES Plasticity in Binding Confers Selectivity in Ligand-Induced Protein Degradation. Nat. Chem. Biol 2018, 14 (7), 706–714. 10.1038/s41589-018-0055-y. [PubMed: 29892083]

(36). Douglass EF; Miller CJ; Sparer G; Shapiro H; Spiegel DA A Comprehensive Mathematical Model for Three-Body Binding Equilibria. J. Am. Chem. Soc 2013, 135 (16), 6092–6099. 10.1021/ja311795d. [PubMed: 23544844]

(37). Nawrocki ST; Griffin P; Kelly KR; Carew JS MLN4924: A Novel First-in-Class Inhibitor of NEDD8-Activating Enzyme for Cancer Therapy. Expert Opin. Investig. Drugs 2012, 21 (10), 1563–1573. 10.1517/13543784.2012.707192.

(38). Baltrushis RS; Beresnevichyus Z-IG; Vizgaitis IM 1-Phenyl-5(6)-Methyldihydrouracils and Their Transformations. Chem. Heterocycl. Compd 1981, 17 (8), 816–820. 10.1007/BF00503666.

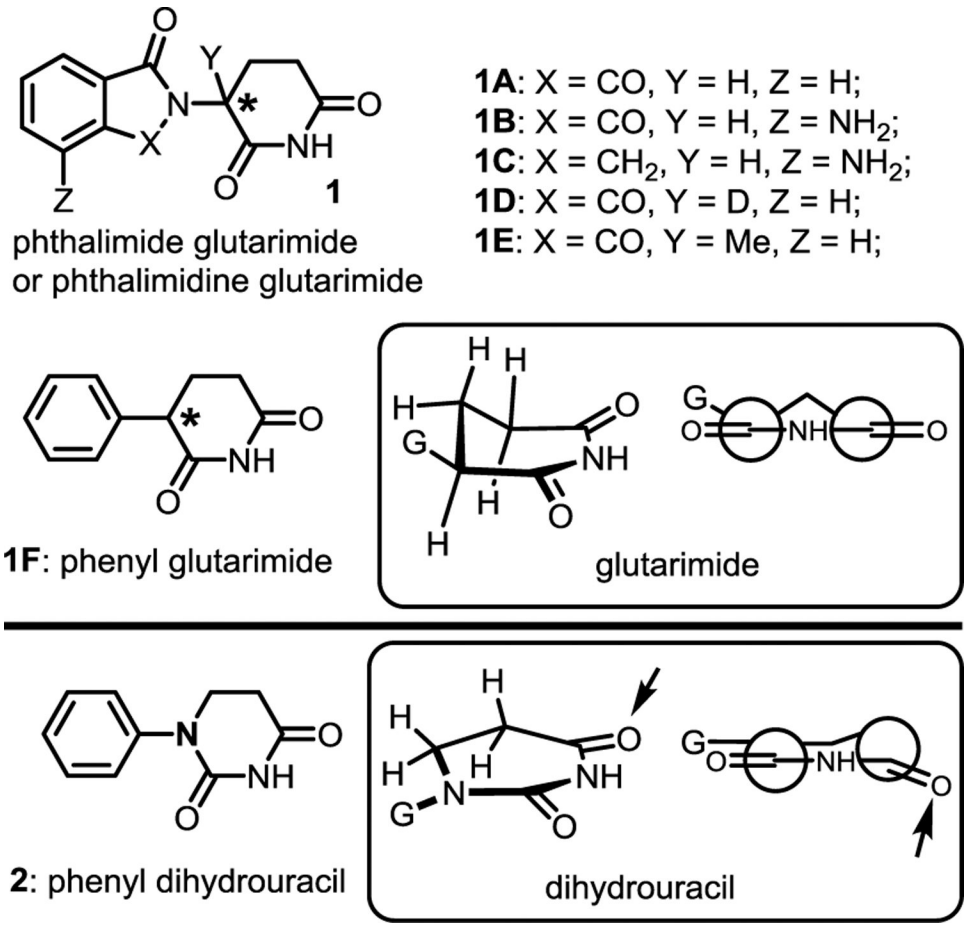

Figure 1.

Comparison of the well-known glutarimides,[13,14] the recently reported phenyl glutarimide,[28] and the designed achiral phenyl dihydrouracil.

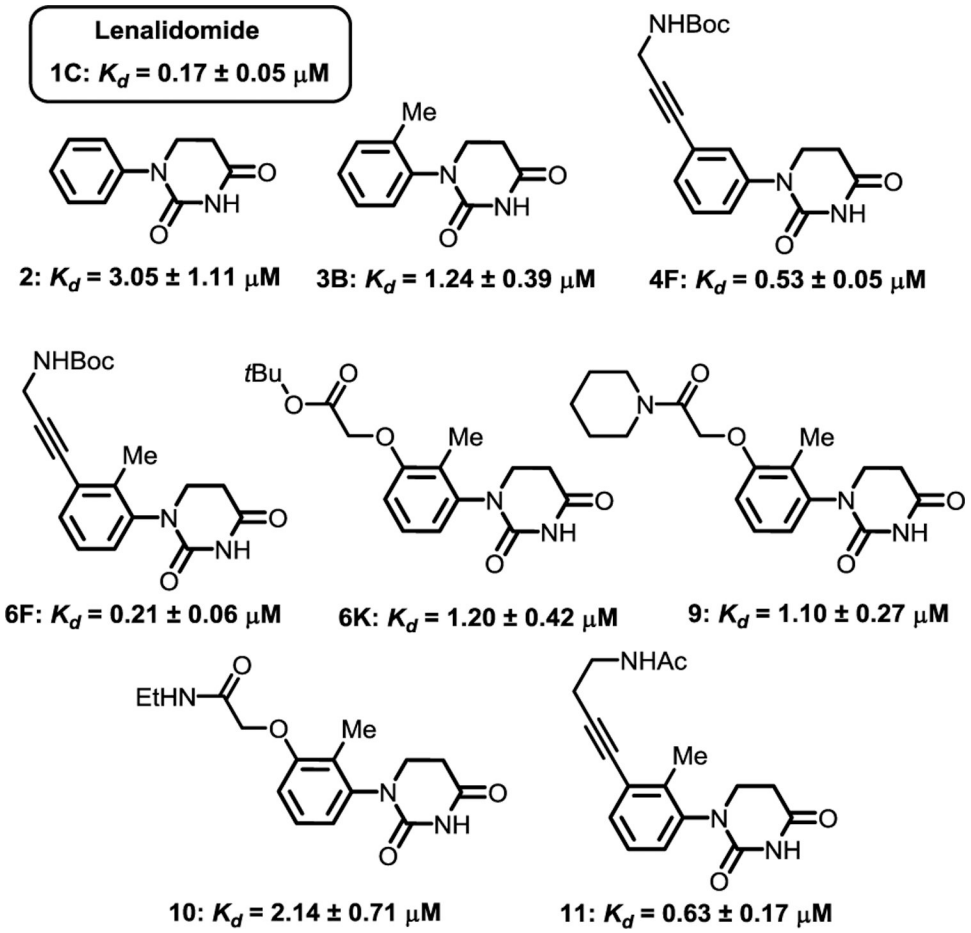

Figure 2.

Binding affinities of lenalidomide and selected PDHUs in a fluorescent polarization assay. (Detailed procedures are provided in the SI.)

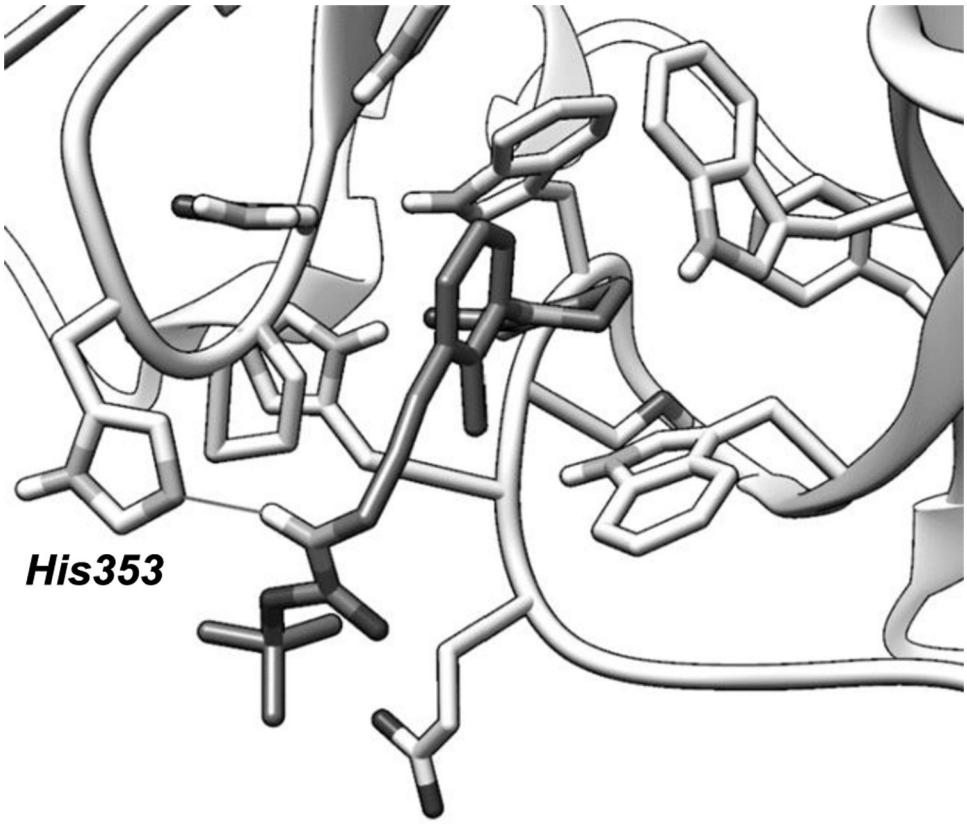

Figure 3.

Binding poses of **6F** based on computational modeling. The dark sticks are from 6F and a key H-bond between the amide and histidine is marked out with a straight line. Image generated by UCSF Chimera.

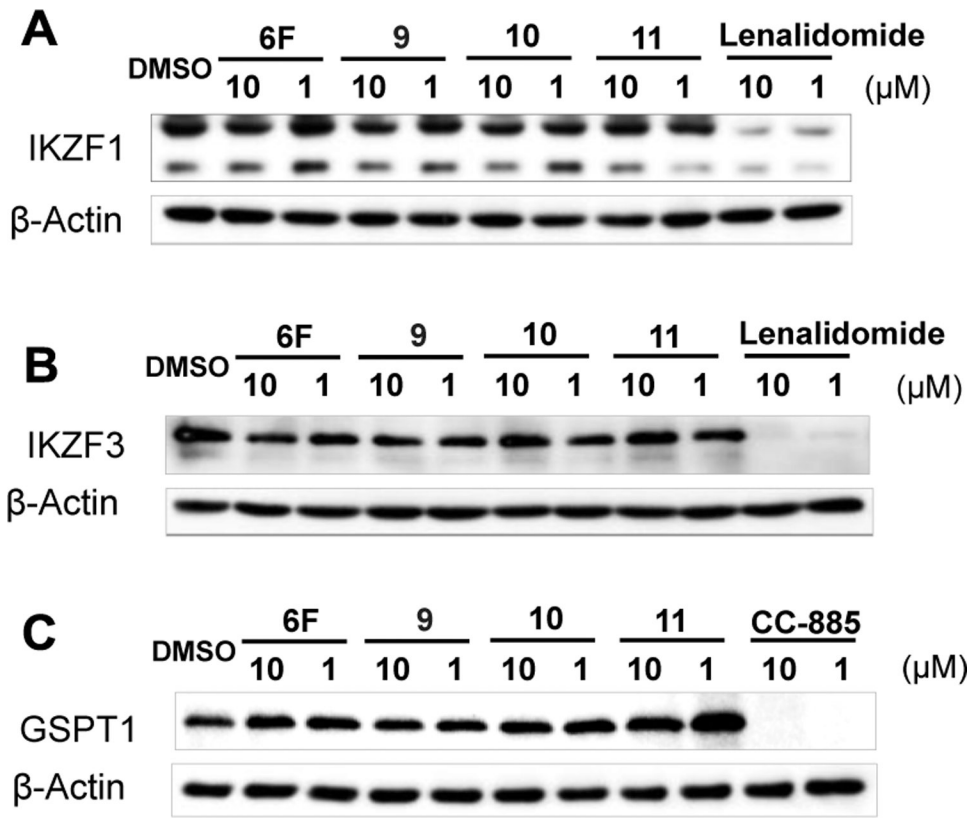

Figure 4.

Compounds **6F**, **9**, **10** and **11** do not induce the degradation of IKZF1, IKZF3 or GSPT1. (A), (B) and (C) Western blots of IKZF1, IKZF3 and GSPT1. MV4;11 cells were treated with **6F**, **9**, **10**, **11**, Lenalidomide or CC-885 at 10 and 1 μM for 24 h.

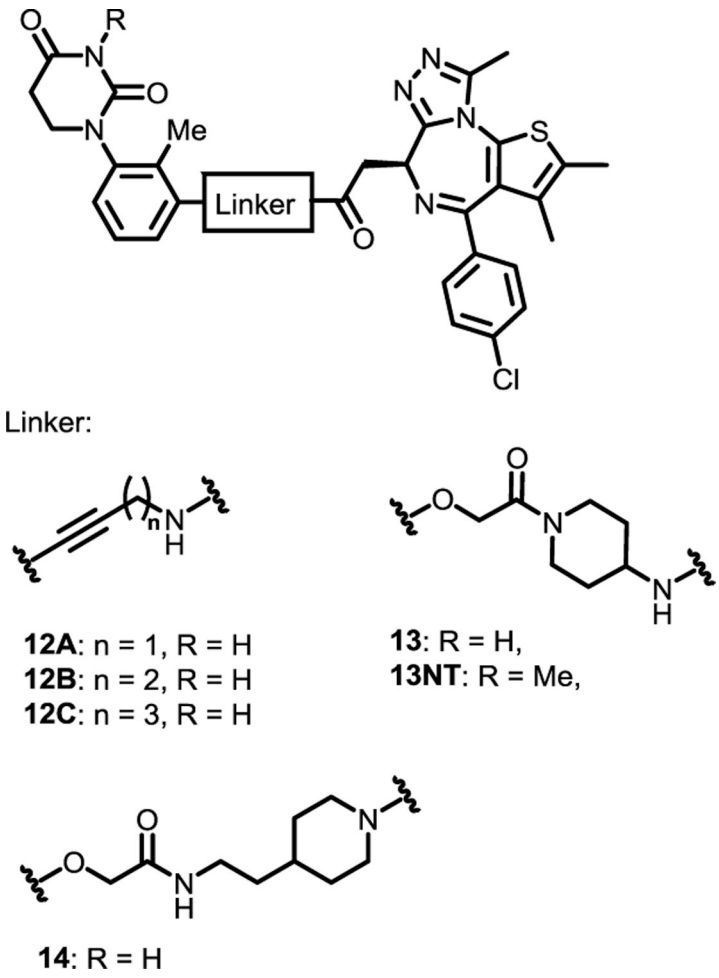

Figure 5.
BRD4 degraders with achiral CRBN ligands

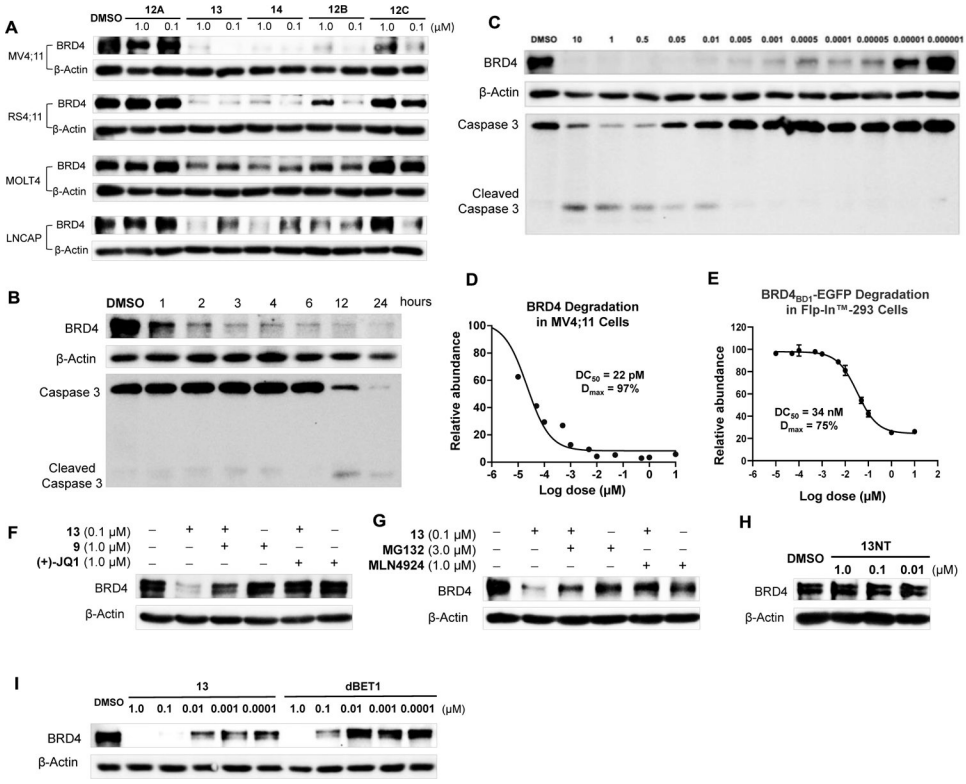

Figure 6.

(A) Western blot of BRD4. MV4;11, RS4;11, MOLT4 and LNCaP cells were treated by **12A, 12B, 12C, 13 and 14** at 1.0 and 0.1 μM for 24h. (B) Time course based on Western blot of BRD4, caspase 3 and cleaved caspase 3. MV4;11 cells were treated by **13** with indicated time. (C) and (D) Dose responses based on Western blot of BRD4, caspase 3 and cleaved caspase 3. MV4;11 cells were treated by **13** with indicated concentrations for 24 h. DC_{50}: the concentration where 50% of the protein has been degraded. D_{max}: the maximum degradation that can be achieved. (E) Quantitative assessment of degradation using a $BRD4_{BD1}$ -e-GFP reporter assay. Dose response based on fluorescent signal ratio of e-GFP to mCherry. Flp-In™-293 Cell Line was treated with **13** at indicated concentrations for 24 h. (F), (G) and (H) Confirmation of mechanism of action by Western blot of BRD4. For (F) and (G), MV4;11 cells were pretreated by JQ1, **9**, MG132 or MLN4924 for 1 h followed by the treatment of **13** for 3 h. For (H), MV4;11 cells were treated by 13NT at indicated concentrations for 24 h. (I) MV4;11 cells were treated by **13** or dBET1 with indicated concentrations for 24 h.

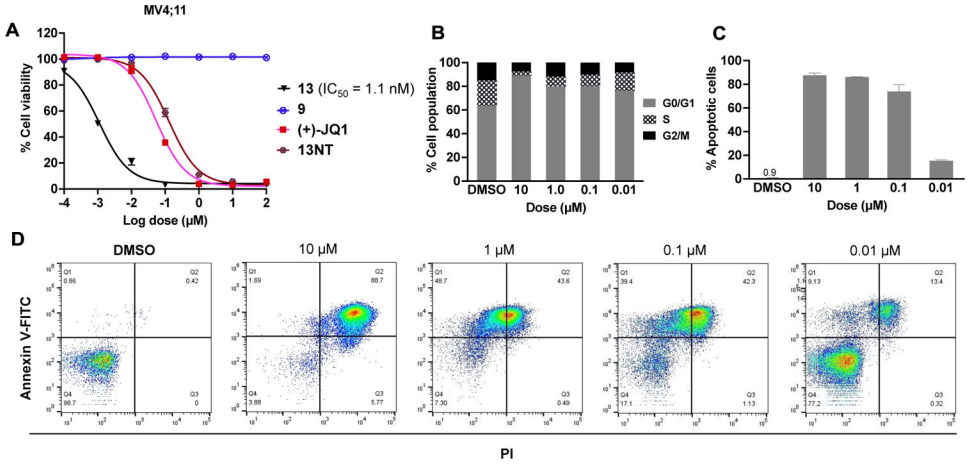

Figure 7.

Functional studies of the PROTACs on cell viability, cell cycle progression and cell apoptosis. (A) AlamarBlue™ Cell Viability. MV4;11 cells were treated by **13**, **9**, (+)-JQ1 and **13NT** for 72 h. (B) MV4;11 cells were treated by indicated dosage of **13** for 48 h followed by flow cytofluorimetric cell cycle analysis. (C) and (D) MV4;11 cells were treated by indicated dosage of **13** for 48 h followed by flow cytofluorimetric apoptosis analyses.

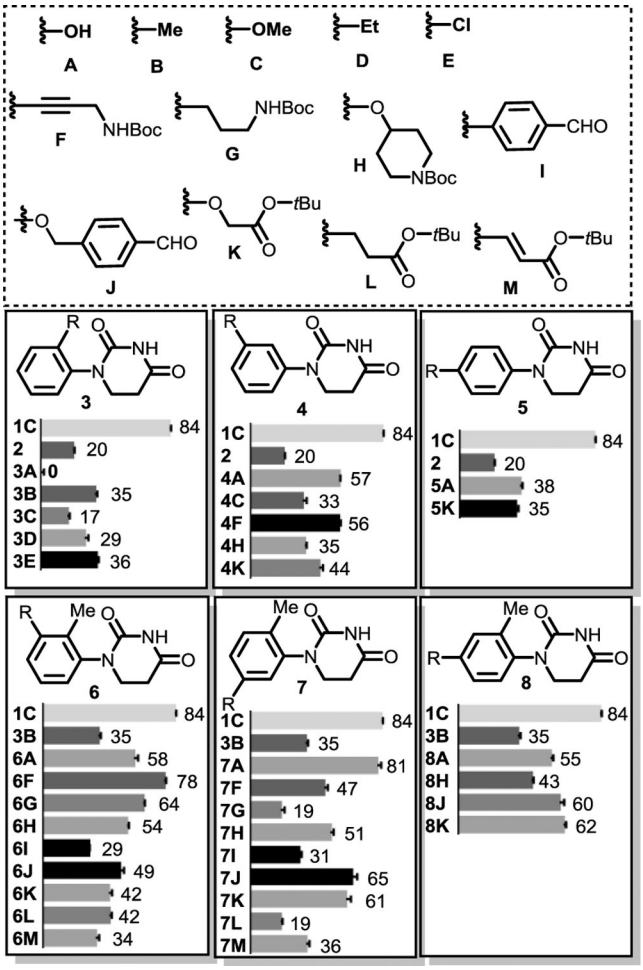

Scheme 1.

Relative binding affinities of substituted PDHUs in a fluorescent polarization assay. Lenalidomide **1C** was used as the positive control and each compound was tested three times.

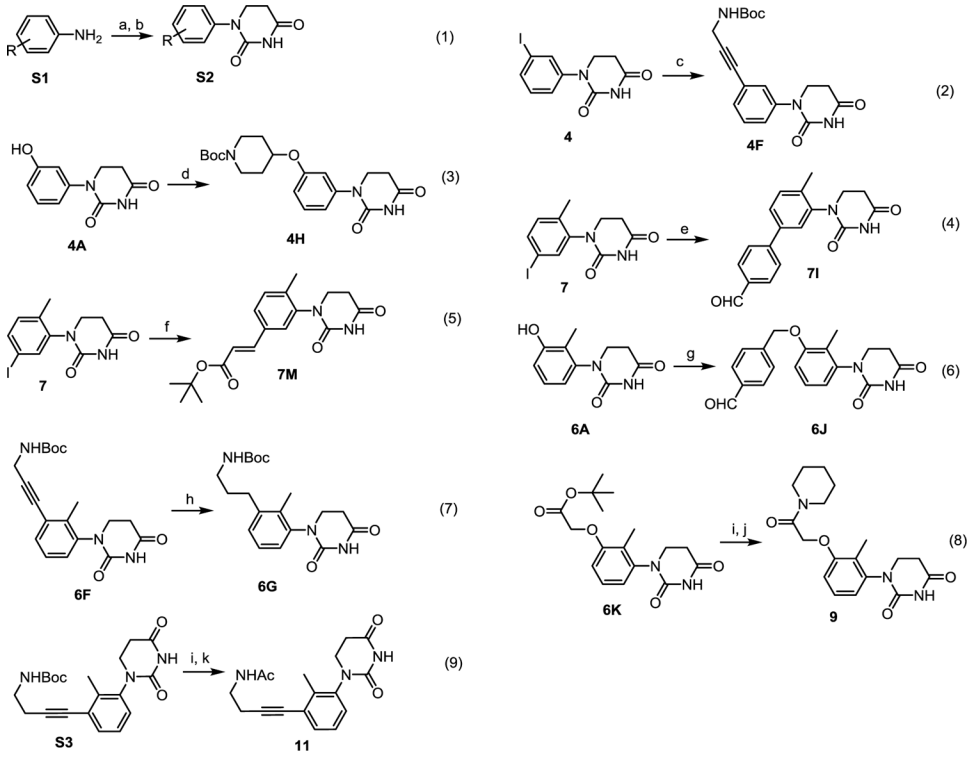

Scheme 2.

The synthesis of achiral CRBN ligands and BRD4 degraders. Reagents and conditions: (a) Acrylic acid, toluene, 110 °C; (b) Urea, acetic acid, 120 °C, (a) and (b) total yield 33%; (c) *N*-Boc-propargylamine, $Pd(PPh_3)_2Cl_2$, CuI, DMF, NEt_3, rt, yield 75%; (d) 1-Boc-4-bromopiperidine, K_2CO_3, Acetonitrile, 110 °C, yield 31%; (e) 4-Formylphenylboronic Acid, $Pd(dppf)Cl_2$, KOAc, DMSO, 90 °C, yield 43%; (f) *tert*-Butyl acrylate, $Pd(OAc)_2$, P(*o*-tol)$_3$, NEt_3, DMF, 110 °C, yield 61%; (g) 4-(Chloromethyl)benzaldehyde, K_2CO_3, Acetonitrile, 60 °C, yield 24%; (h) Pd/C, H_2, MeOH, rt, yield 95%; (i) TFA/DCM, rt, yield 95%; (j) Piperidine, HATU, DIPEA, DMF, rt, yield 82%; (k) Ac_2O, NEt_3, DMF, rt, yield 64%.

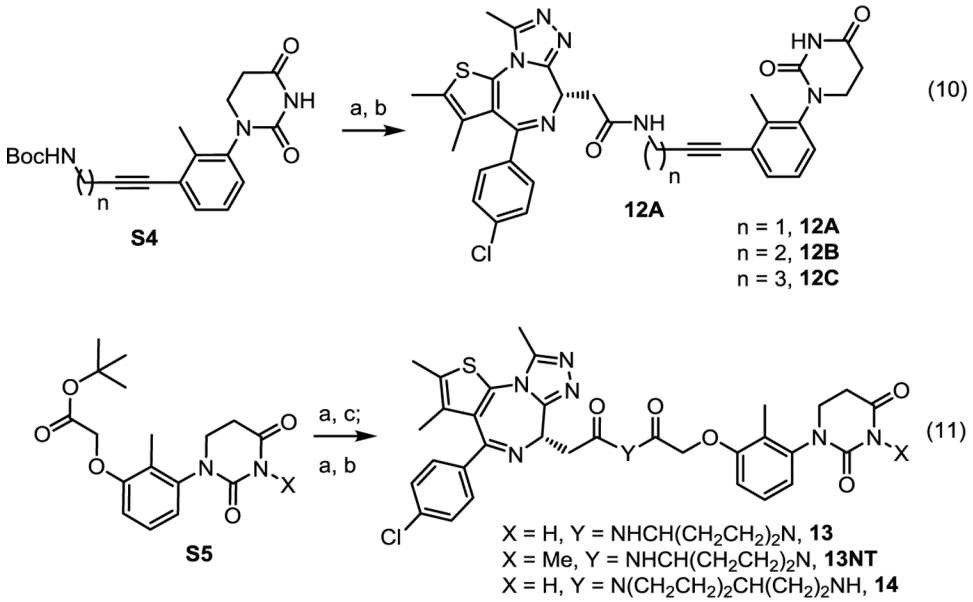

Scheme 3.

The synthesis of BRD4 degraders using achiral CRBN ligands. Reagents and conditions: (a) TFA/DCM, rt; (b) JQ-1 (carboxylic acid), HATU, DIPEA, DMF, rt, (a) and (b) total yield 86%; (c) 4-(*N*-Boc-amino)piperidine (or 4-(Aminoethyl)-1-*N*-Boc-piperidine), HATU, DIPEA, DMF, rt, yield 80%.

Table 1.

Stability of lenalidomide and 1,2,3-trisubstituted PDHUs

Compound	hLM[a]	hP[b]	pH=1.0[c]	pH=7.4[d]	pH=8.8[e]
Lenalidomide	89	62	>99	39	0, 20[f]
6F	87	97	>99[g]	>99	93
9	85	81	>99	>99	95
10	100	88	>99	>99	95
11	90	102	>99	>99	90

[a] Percent compound remaining after 0.5 h.

[b] Percent compound remaining after 4.0 h.

[c-e] Glutarimides and dihydrouracil ring opening hydrolysis, percent compound remaining after 24 h.

[f] Percent compound remaining after 2 h.

[g] Boc was deprotected, dihydrouracil ring opening hydrolysis was not detected by LC-MS. (Detailed procedures are provided in the SI.)